Preprint Cambridge Centre for Computational Chemical Engineering ISSN 1473 – 4273

Evolution of the soot particle size distribution along the centreline of a *n*-heptane/toluene co-flow diffusion flame

Jochen A.H. Dreyer[1,4], Maximilian Poli[1], Nick Eaves[1], Maria L. Botero[2], Jethro Akroyd[1,4], Sebastian Mosbach[1,4], Markus Kraft[1,3,4]

released: 13 August 2018

[1] Department of Chemical Engineering
and Biotechnology
University of Cambridge
Philippa Fawcett Drive
Cambridge, CB3 0AS
United Kingdom

[2] Department of Mechanical Engineering
National University of Singapore
9 Engineering Drive
117576
Singapore

[3] School of Chemical
and Biomedical Engineering
Nanyang Technological University
62 Nanyang Drive
637459
Singapore
E-mail: mk306@cam.ac.uk

[4] Cambridge Centre for Advanced Research and
Education in Singapore (CARES)
CREATE Tower, 1 Create Way
138602
Singapore

Preprint No. 206

Keywords: Soot, laminar diffusion flame, liquid fuel, toluene/heptane, particle size distribution

Edited by
Computational Modelling Group
Department of Chemical Engineering and Biotechnology
University of Cambridge
West Cambridge Site
Philippa Fawcett Drive
Cambridge CB3 0AS
United Kingdom

Fax: + 44 (0)1223 334796
E-Mail: c4e@cam.ac.uk
World Wide Web: http://como.cheng.cam.ac.uk/

Abstract

A newly developed experimental set-up for studying liquid hydrocarbon combustion in the well-established Yale burner was used to investigate the correlation between fuel composition and its sooting propensity. Soot particle size distributions (PSDs) and flame temperatures along the centreline of an *n*-heptane/toluene co-flow diffusion flame are reported. The addition of toluene (0, 5, 10, and 15 mol%) to heptane moved soot inception to lower heights above the burner (HAB). The earlier inception extended the soot growth zone in the toluene-laden flames, leading to larger soot primary and agglomerate particles. Toluene addition had little influence on the maximum soot number density, indicating that increases in soot volume fraction can mainly be attributed to the observed increase in particle size. In order to explain the reasons for earlier soot inception in the presence of toluene, fuel decomposition and PAH formation were simulated in a perfectly-stirred reactor, with conditions corresponding to the fuel-rich regions at low HAB. Combining the experimental results with this simple model shows that one- and two-ring species form significantly faster in the presence of toluene, explaining the higher sooting propensity of aromatic fuels. The reported PSDs inside a vapour-fed diffusion flame are the first of their kind and provide a comprehensive dataset for future studies of combustion chemistry and soot particle models.

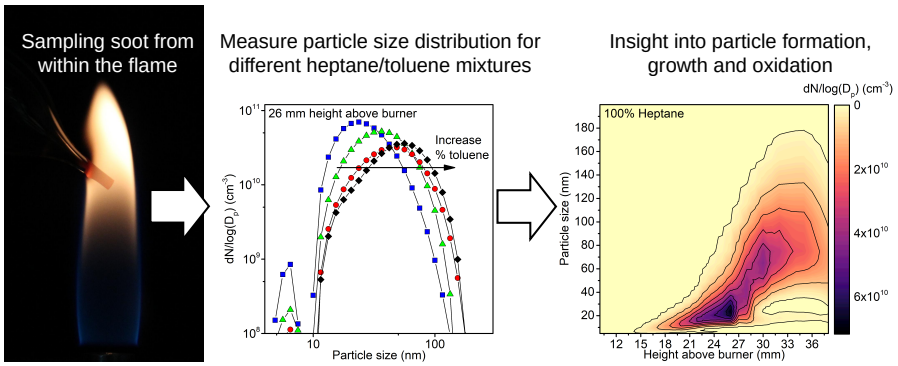

Highlights

- Influence of heptane/toluene mixture on soot formation in a vapour-fed co-flow diffusion flame (Yale burner) was studied
- Newly developed quartz probe to take soot samples from within the flame
- Particle size distributions along the centreline were measured
- Toluene leads to earlier soot nucleation and growth to larger particles
- No influence of toluene on particle number densities

Contents

1 Introduction

Soot formed by incomplete combustion of hydrocarbons has adverse effects on human health [27] and is a major contributor to anthropogenic climate change [20, 23, 39]. However, useful carbonaceous particles such as carbon black are also prepared through combustion on an industrial scale and are used as rubber filler for tire reinforcement [37], additive for electrically conductive polymers [22], or electrode material in batteries [3, 48]. The aim of soot research is to gain a fundamental understanding of the chemical reactions, inception process and PAH clustering, and soot growth leading to soot formation in practical applications. Such an understanding could then be used to mitigate soot emission and enhance the efficiency during energy conversion (internal combustion engines, jet engines, gas turbines, etc.) or to produce tailor-made carbonaceous nanoparticles for industrial applications. In this context, investigating soot formation in laminar flames using aliphatic and aromatic fuel mixtures encountered in real combustion systems is an important area of research [17, 35, 43].

Traditionally, soot research in laminar flames has focused on gaseous fuels because they are easy to handle, with ethylene being amongst the most common choices [7, 25, 30, 42]. In order to study more realistic fuels, less sooty methane flames have been used and doped with small amounts of aromatics and aliphatics [13, 15]. This approach was used to quantify the sooting propensity of a range of aliphatics [15], aromatics [33], and oxygenated [32, 34] fuels by measuring the maximum soot volume fraction inside the doped methane flame. The maximum soot volume fraction can hereby be measured using laser-induced incandescence [32–34] or flame pyrometry [13–15] and converted into apparatus-independent yield sooting indices (YSIs) [32]. McEnally and Pfefferle [31] also doped five different one-ring aromatics (benzene, toluene, ethylbenzene, styrene, phenylacetylene) into a methane diffusion flame and illustrated the importance of the side chain attached to the phenyl ring (H, CH_3, $CH{=}CH_2$, or $C{\equiv}CH$). Their experiments indicated that the naphthalene concentration and soot volume fraction are proportional, making naphthalene formation a crucial step in polycyclic aromatic hydrocarbon (PAH) growth from aromatic fuels [31]. Other researchers linked the amount of key species (benzene, pyrene, acetylene) to the onset and rate of soot inception [44]. Differences in the type and quantity of such species ultimately reflected in the soot number density and size of the soot particles [6, 12, 44]. Adding aromatics such as *n*-propylbenzene to *n*-dodecane/methane diffusion flames was reported to result in earlier soot inception and increased soot number density [49]. Similarly, the addition of toluene to a methane diffusion flame caused a significant increase in the soot volume fraction compared to *n*-heptane addition [12].

Research on pure liquid fuel combustion is less common, partly due to experimental difficulties. One of the simplest set-ups to study liquid fuels is the wick-fed diffusion flame. Such flames have mainly been used to measure smoke points of fuels to assess the fuel's sooting propensity and to calculate apparatus-independent sooting indices,

such as the threshold soot index (TSI) [8] or oxygen extended sooting index (OESI) [4]. Using wick-fed flames to measure smoke points is the standard method for characterising kerosine and aviation turbine fuel as specified in ASTM Standard D1322-15e1. This methodology was used to study sooting propensity of fuel surrogates such as heptane and toluene [5, 6] or oxygenated diesel additives such as polyoxymethylene dimethyl ethers [44]. In addition to sooting propensities, this flame was used to measure particle size distributions (PSD) as a function of fuel flow rate using a differential mobility spectrometer and hole-in-tube probe for sampling [5, 6]. The probe design did not allow sampling from within the flame but an increased mean particle size was observed at the flame tip when toluene was added to the wick-fed heptane flame [6]. More recently, a premixed flat flame was fed with pre-vaporised heptane/toluene and PSDs were measured using the burner stabilised stagnation (BSS) approach [44]. Hereby, the hole-in-tube sampling line is incorporated into the stagnation plate, enabling the sampling of stagnation flames with minimal flame perturbation [2]. The study showed that in premixed flames containing toluene, soot nucleation starts earlier while larger soot particles and volume fractions were detected in the heptane fed flame [44]. One drawback of the BSS is that the soot evolution from the burner surface to the stagnation point can not be studied. Only information about the soot at the stagnation point is retrieved. However, there remains a lack of experimental data in well-defined laminar flames using more realistic fuels such as pre-vaporised heptane as also recognised during the International Sooting Flame (ISF) workshop 2018 [1]. Having PSDs inside such flames would further extend the recent efforts to simulate PSDs in ethylene-fed BSS flames [29, 36, 46] to more realistic fuel surrogates.

The **purpose of this study** is to provide a comprehensive dataset of soot PSDs (as opposed to averaged sizes or volume fractions) inside a well-defined liquid-fueled co-flow diffusion flame. Four different fuel mixtures containing heptane and toluene were studied to evaluate the influence of aromatics on the evolution of particle size and number along the centreline of the flame. The soot was sampled using a newly developed quartz probe that facilitated the monitoring of the entire soot evolution process, starting with soot nucleation, followed by growth, aggregation and agglomeration, and finally soot oxidation. The presented experimental and numerical results explain why toluene has a higher sooting propensity and how it reflects in the PSD evolution. The PSD dataset is attached in the supporting information to provide a reference for the soot community and to test the various soot particle models used in literature [26, 29, 36, 45–47].

2 Materials and methods

2.1 Co-flow diffusion flame

A new experimental flame set-up was developed to study vapour-fed co-flow diffusion flames (Fig. 1a). A syringe pump (New Era NE-501) delivered 7 g h^{-1} of fuel to an evaporator (Bronkhorst CEM). Here, the fuel was mixed with 200 mL min^{-1} Ar (Bronkhorst El-Flow) and evaporated. The fuel/carrier gas mixture was passed through heated lines (150 °C) to the central 1/4" stainless steel tube (inner diameter 0.218") of a Yale burner [13, 14]. Compressed air at 50 L min^{-1} (Bronkhorst El-Flow) was used for the co-flow through a 3" stainless steal honeycomb mesh (0.017" wire diameter, 18x18 mesh). The burner was mounted on a vertical translational stage (Festo) with a positioning accuracy of 0.1 mm.

In this study, four different fuel mixtures (pure heptane, and 5, 10, and 15 mol% toluene in heptane) were used. The required volumetric quantities of *n*-heptane (VWR, 99.8 %) and toluene (Sigma-Aldrich, 99.8 %) were calculated based on the desired mol% composition. The densities of the mixtures required for the syringe pump were determined experimentally by measuring the mass of a known volume of fuel.

2.2 Flame temperature

The flame temperatures were measured with a S-type thermocouple having a wire diameter of 0.2 mm and microscopically measured bead size of 0.6 mm. Two pull-action computer-controlled solenoids enabled the rapid insertion and removal of the thermocouple to/from the flame. Temperatures were measured over 60 s to detect the height above the burner (HAB) at which soot starts to form. In the presence of soot, the deposition of soot on the thermocouple causes the measured temperature to decrease over time due to an increasing emissivity and bead size [16]. After each temperature measurement, the thermocouple was placed above the flame tip to burn off any soot deposits. The temperature extrapolated to $t = 0$ s was used as the thermocouple junction temperature T_j. It was corrected for emission to obtain the gas temperature T_g [41]:

$$T_g = T_j + \varepsilon_j \cdot \sigma \frac{(T_j^4 - T_w^4)d}{k \cdot Nu} \tag{1}$$

The temperature junction emissivity ε_j was calculated with the reported cubic polynomial for S-type thermocouples [41] while Nu was calculated for a cylindrical profile [18]. T_w is the ambient temperature, σ is the Stefan-Boltzmann constant, and k is the thermal conductivity of the gas. The mapping of the centreline temperature was repeated 7 times and calculated gas temperatures were averaged.

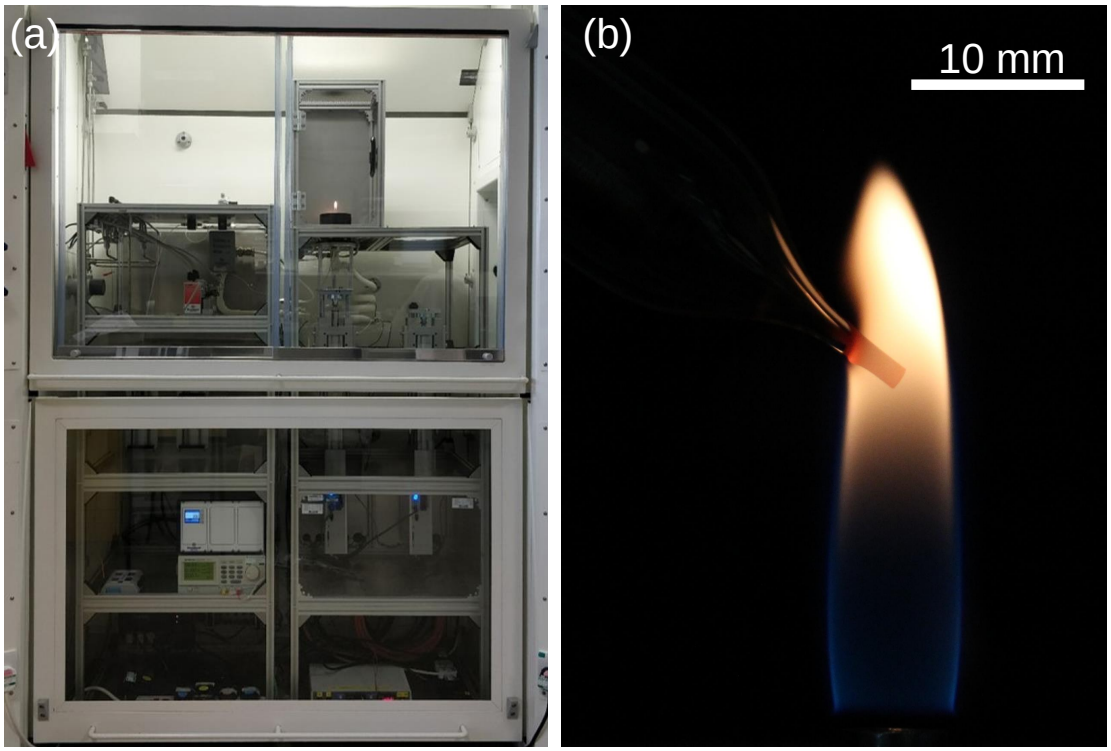

Figure 1: *Left: Experimental flame set-up for the vapour-fed co-flow diffusion flame. Right: Soot sampling using a quartz tube with a 0.4 mm orifice.*

2.3 Soot particle size and number

Soot samples from flames are most commonly taken with a hole-in-tube probe, i.e., a stainless steel tube having a small orifice to draw in a sample [9–11, 24, 50]. Previous studies have used such probes to sample soot from the flame tip as well as from within flames, and risk significantly perturbing the flame with respect to the flow field and temperature profile [9, 50]. In this study, a newly developed sampling probe based on the report by Hepp and Siegmann [21] was used to take soot samples from within the flame. Advantages over the hole-in-tube approach are a reduced flame disturbance when sampling from within the flame and that the probe geometry induces enhanced mixing between the sample and diluent [19, 21]. Except the quartz tube, all parts required for assembling the sampling probe are standard fittings. A technical drawing of the design as well as the part numbers of the used fittings are provided at the end of the supporting information.

The quartz tube used for soot sampling had an outer diameter of 12 mm, inner diameter of 8 mm, and a tip with a 0.4 mm pinhole (Fig. 1b). The geometry of the tip was developed to minimise flame disturbance and residence time of the sample in the tip

before mixing with the diluent. Immediately after the tip, the sample was diluted with approx. 8.5 L min^{-1} N_2 and sucked into a central 6 mm stainless steel tube. The exact N_2 flow rate was adjusted to achieve the same flow rate through the nozzle in each experiment. The dilution ratio in the probe was in the range 170–250 for all experiments. However, the exact ratio was not constant because it changed depending on the temperature at the probe tip, progressive clogging of the orifice in highly sooting regions of the flame, and limitations of the DMS500 mass flow meters (see below). The diluted sample was passed through a conductive silicon tube to a Differential Mobility Spectrometer (Cambustion DMS500), where a further dilution by a factor of 500 was achieved with a rotating disc diluter.

At each HAB, the particle size distribution was recorded for 15 s at a rate of 10 Hz and averaged. Each experiment was repeated four times and error bars are reported as min/-max values to indicate the reproducibility of the experiments. A log-normal function was fitted to the measured curves to deconvolute bimodal particle size distributions and to obtain the size and number density of each mode.

3 Results and discussion

The fuel, carrier gas, and sheath air flow rates were chosen such that all flames are slightly lifted (1–1.5 mm, Fig. 2) to minimise heat transfer into the fuel tube and to simplify the boundary conditions in any future numerical simulations. The luminescent flame height of the *n*-heptane flame is 37 mm. Adding toluene to the fuel mixture successively increases the flame height (41 mm for 15 mol% toluene) and elongates the yellow luminescence zone towards lower height above burner (HAB). A shift of the luminous zone towards lower HAB and elongation of the flame with increasing aromatic content is in agreement with previous reports where *n*-propylbenzene was added to a *n*-dodecane/methane diffusion flame [49]. The given explanation was earlier soot inception and increased time before complete soot oxidation [49].

The temperatures of the four flames are almost identical at low HAB, increasing from 860 K at 3 mm HAB to 1260 K at 17 mm HAB (Fig. 3). At 15 mm HAB, the temperatures start to diverge slightly with the pure heptane flame reaching slightly higher temperatures. At 23 mm HAB, all flames show a local maximum. Above 27 mm HAB, the divergence in flame temperatures becomes more pronounced. All flames reach a local temperature minimum around 27–29 mm HAB after which the temperatures start to increase again. The temperature difference between the heptane and toluene-containing flames is up to 350 K at 31 mm HAB, indicating substantial differences in the flame chemistry or heat radiation. It is assumed that the slightly lower flame temperatures of the toluene containing flames between 15–27 mm HAB are caused by a higher soot volume fraction, causing an increase in the radiative cooling. The drop in temperature above 23 mm HAB and local minimum at 27–29 mm HAB indicates a high soot vol-

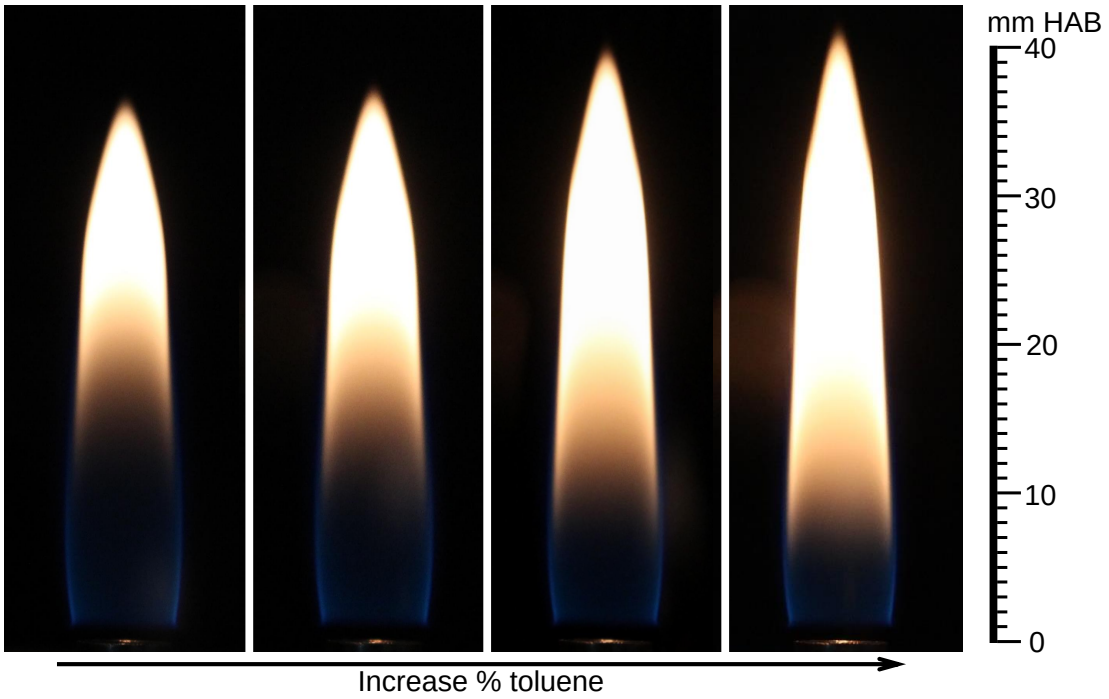

Figure 2: *Photographs of the co-flow diffusion flames fed with four different fuel compositions but identical fuel mass flow rates. From left to right: pure n-heptane, 5 mol% toluene/heptane, 10 mol% toluene/heptane, 15 mol% toluene/heptane.*

ume fraction in these regions, leading to substantial cooling due to radiative heat loss. This would also be in agreement with the higher temperature drop of the sootier toluene containing flames. The maximum temperature of the heptane flame is at 33 mm HAB (1792 K), while adding toluene reduces the maximum temperature (1716 K for 5 % toluene) and shifts the maximum towards larger HAB (37 mm HAB).

The transient thermocouple response can give a qualitative impression of the HAB at which soot starts to form. For the heptane flame, the temperature remains constant at 11 mm HAB and decreases as a function of time at 13 mm HAB (Fig. S2). The decrease in temperature is hereby caused by soot deposition on the thermocouple, causing its emissivity and bead size to increase [16]. The addition of toluene causes a time dependent temperature decrease at lower HAB, indicating earlier soot inception. The earlier soot formation with increasing toluene concentration explains the shift of the luminescence zone towards lower HAB as observed in Fig. 2 and is in agreement with previous reports [31, 44].

Exemplary particle size distributions inside the flame measured with a differential mobility spectrometer (DMS) are shown in Fig. 4 as log-log plots. The full data set can

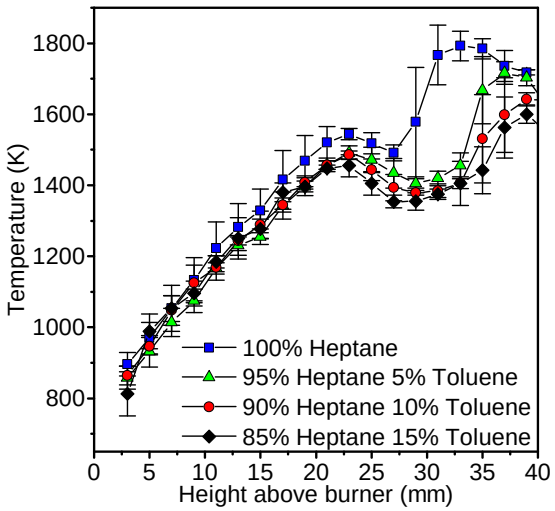

Figure 3: *Measured centre line flame temperatures as a function of HAB and fuel composition. The error bars show the 95% confidence interval.*

be found in the Supporting Information, Tables S2–S5. At 10 mm HAB, an increase in the toluene content leads to more soot particles while at higher HAB, the particle size distribution seems to be shifted towards larger particles. Contour plots with a linear scale for $dN/dlogD_p$ are shown in Fig. 5 as they illustrate the key trends most clearly. The onset of soot formation as determined using the DMS (Fig. 5) indicates that soot starts to form earlier in the flame as the toluene content is increased. This is in good qualitative agreement with the elongated luminescence zone observed in Fig. 2. For all flames, the size and number of soot particles steadily increases with increasing HAB up to about 26 mm HAB. Thus toluene addition does not simply shift the reaction zone towards lower HAB but extends the time for soot formation and growth prior to oxidation. Above 26 mm HAB, the particles continue to increase in size and the PSD starts to become bimodal (also see Fig. 4c). At increasing HAB, the soot particles continue growing in size with toluene leading to notably larger particles. Most soot is oxidised by 40 mm HAB for the heptane flame but not for the 15 mol% toluene containing flame, explaining the increased flame height with increasing toluene content observed in Fig. 2. It is worth noting that the luminescent flame height is simply the point where a clear signal was detected with the given camera setting and is therefore not identical with the point where all soot is oxidised.

The averaged mean particle size and number densities give a more quantitative insight into the soot evolution inside the four flames (Fig. 6). In case of a bimodal PSD, the two modes are referred to as major (Fig. 6a and b) and minor mode (Fig. 6c and d) based on the number of soot particles they contain. For the heptane flame, the first soot particles can be observed around 15 mm HAB while toluene addition results in earlier soot nucleation (9 mm HAB for 15 mol% toluene). This onset of soot formation

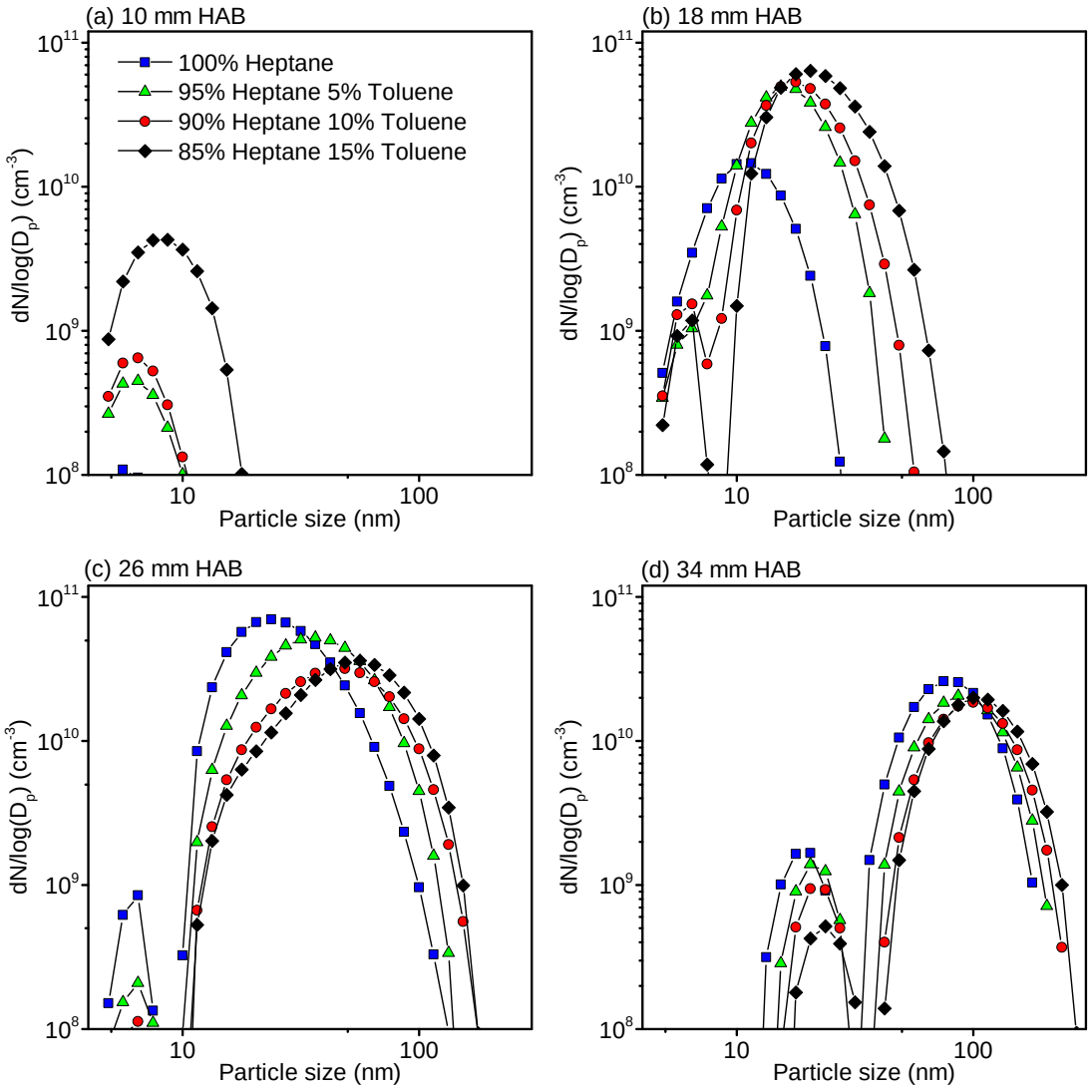

Figure 4: *Particle size distributions inside the four studied diffusion flames at (a) 10 mm HAB, (b) 18 mm HAB, (c) 26 mm HAB, and (d) 34 mm HAB.*

agrees well with the HAB at which soot deposition starts to cause the thermocouple temperature to decrease with time (Fig. S2). As intrusive techniques and insufficient sample dilution would shift the soot formation towards lower HAB [21, 40], the results indicate good sample quenching and minimal coagulation in the sampling lines. With increasing HAB, the size and number of the soot particles increase steadily up to 25 mm HAB for the heptane flame and 20 mm HAB for the 15 mol% toluene flame (Fig. 6a and b). At 15–21 mm HAB, the particle size distribution shifted towards larger sizes and another mode with average size of 7 nm becomes visible (Fig. 6c and d). It is probable that this minor mode is also present at lower HAB but is obscured by the

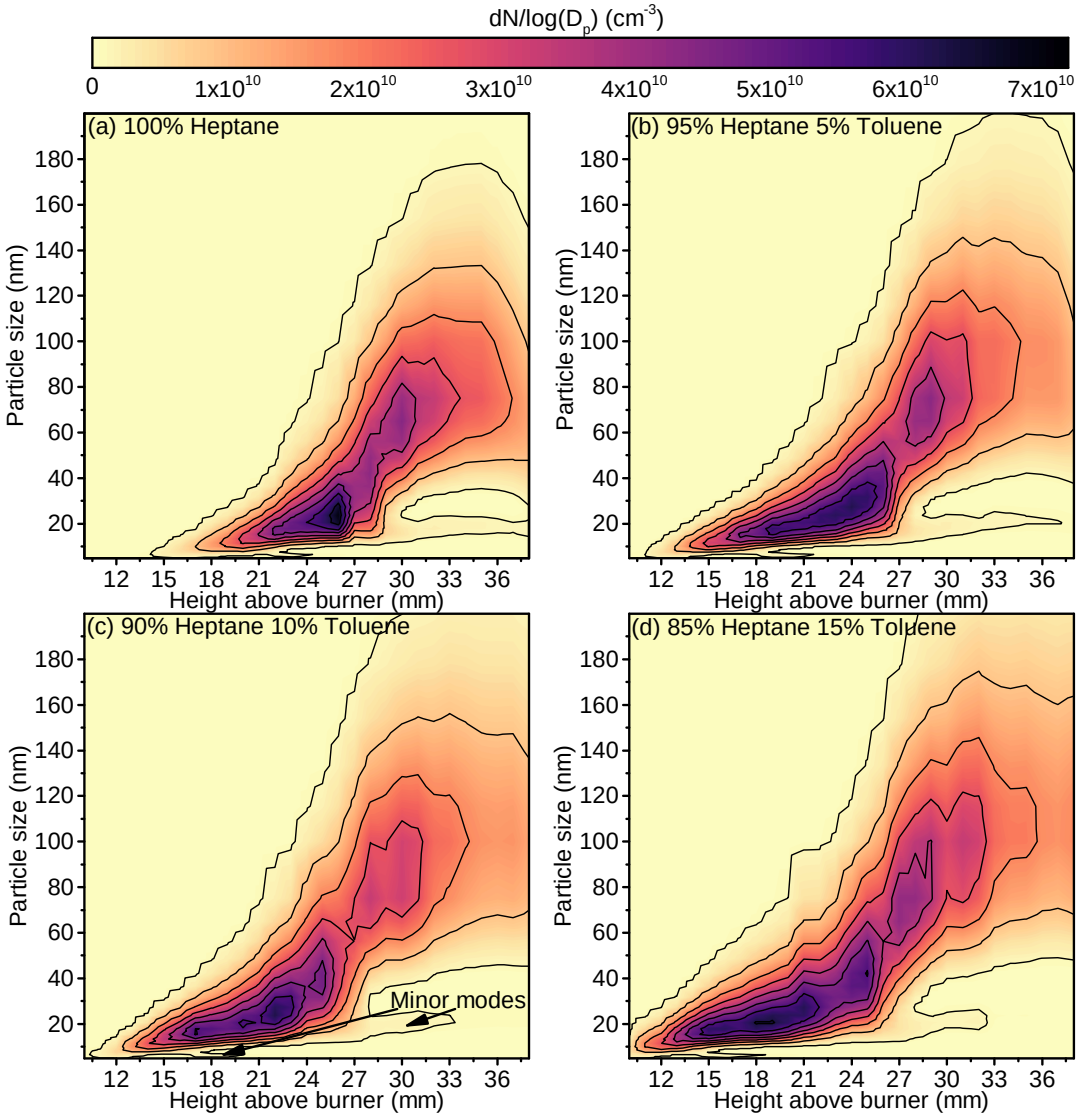

Figure 5: *Measured particle size distribution as function of height above burner and fuel structure. The minor mode discussed in the text and quantified in Fig. 6 is indicated in (c).*

major mode. The number density of this minor mode decreases with HAB (Fig. 6d), suggesting its consumption by coalescence or aggregation with other particles. The frequently reported inception mode below 5 nm [44, 46, 50] was not observed due to the detection limit of the DMS (∼5 nm).

Following the near linear increase in soot diameter up to 20–25 mm HAB, the particle size increase becomes more rapid (Fig. 6a). Notably, the HAB at which the slope

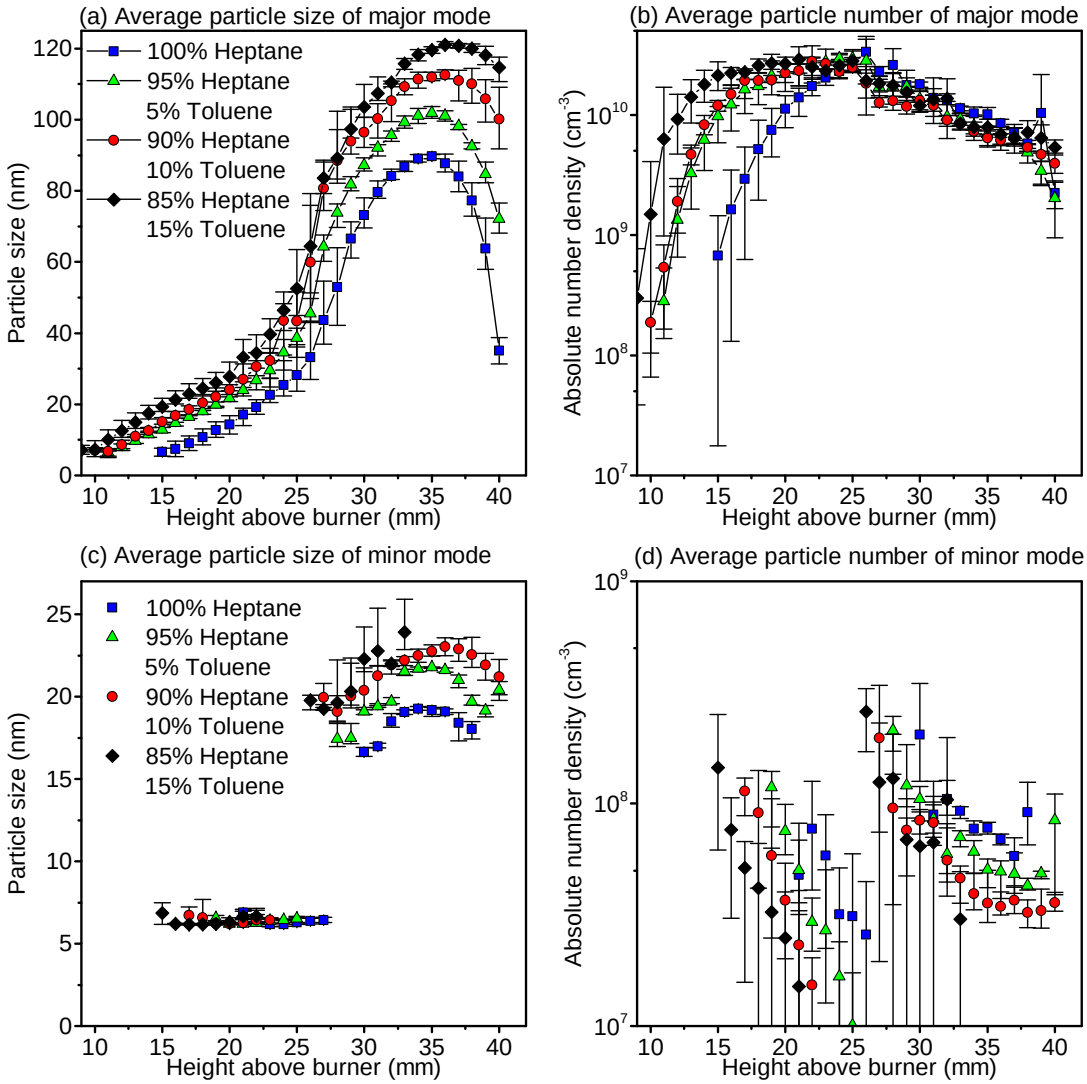

Figure 6: *Particle sizes and number densities of the major and minor modes observed in the particle size distribution. The error bars represent the max. and min. values.*

in particle size growth changes (Fig. 6a) coincides with the HAB of maximum particle number density (Fig. 6b). Thus the rapid increase in particle size is accompanied with a decrease in particle number, suggesting that aggregation and agglomeration now dominate. The maximum size varies significantly with fuel structure, increasing from 90 nm for pure heptane to 121 nm for 15 mol% toluene/heptane. Previous DMS500 measurements at the tip of a wick-fed diffusion flame using *n*-heptane/toluene mixtures as fuel showed a similar trend [6]. At 26–30 mm HAB, the PSD starts to become bimodal and a mode with a size around 20 nm becomes visible (Fig. 6c and d). Similar

to the minor 7 nm mode between 15–27 mm HAB, the 20 nm mode is expected to be obscured at lower HAB. The size range of about 20 nm [6, 28] is in good agreement with the primary particles frequently observed in TEM [6, 7, 28]. The mean size of these primary particles depends on the fuel structure, increasing from about 19 nm for heptane to 24 nm for 15 mol% toluene-heptane. The trend of increasing primary particle size with increasing toluene content was also observed in TEM images of soot sampled from a wick-fed diffusion flame [6]. The HAB at which the primary particles and soot aggregates/agglomerates reach a maximum size is at 35–36 mm for all fuels. Above 36 mm HAB, both the size and the number of particles decrease, indicating that the soot is rapidly consumed by oxidation.

The maximum number density is similar for all flames (Fig. 6b). The key difference between the four fuel mixtures is the HAB at which soot nucleation starts. Soot formed earlier in the flame has more time to grow in size prior oxidation, explaining the larger primary particle size as seen in Fig. 6c. The larger primaries collide to form larger aggregates and agglomerates as seen in 6a. The morphology of these agglomerates/aggregates was not studied here, thus the relationship between soot size and volume fraction or mass is unknown. Assuming spherical particles is an oversimplification but can nevertheless give a rough estimate of the order of magnitude in soot volume change. Keeping the soot number constant but increasing its size from 91 nm (heptane) to 121 nm (15 mol% toluene-heptane) would increase the soot volume by a factor of 2.4. This significant increase in soot volume fraction would cause higher heat loss from the flame due to thermal radiation, which can be observed in Fig. 3.

It is worth noting that the uncertainties in the dilution corrected soot numbers are not caused by changes in the experimental conditions. Notably, the measured particle size distributions remain stable with time (Fig. S3a). The dilution factor recorded by the DMS fluctuated significantly however due to the limitations of the mass flow meters inside the DMS, introducing significant fluctuations into the dilution corrected number densities (Fig. S3b). This explains the relatively small error bars in the mean particle sizes (Fig. 6a and c) but large uncertainties in the number densities (Fig. 6b and d). Therefore, a more accurate method to measure sample dilutions is expected to have the most significant impact on decreasing the experimental uncertainties.

To explain why toluene addition leads to earlier soot inception, simulations of perfectly-stirred reactors (PSRs) with heptane and 15 mol% toluene/heptane at temperatures observed before, during and after soot inception (800, 1000, and 1200 K) were performed (Table S1 and Fig. S4). The PSR was not an attempt to model the centreline of the flame, but to examine the relative chemical (as opposed to mixing) rates of processes that contribute to PAH growth. The chemical mechanism was developed for gasoline surrogates [38] and previously successfully used for modelling soot formation in laminar co-flow diffusion flames of gasoline/ethanol blends [26]. The simulation results indicate that both, toluene and heptane form naphthalene and thus larger PAHs through vinylacetylene (C_4H_4) addition to phenyl radicals and ehtylene (C_2H_4) addition to 2-

ethynylphenyl radicals. However, heptane needs to form aromatics through the cyclisation of linear hydrocarbons while toluene already consists of an aromatic ring. Consequently, the naphthalene precursors phenyl and 2-ethynylphenyl radicals form orders of magnitude faster in the presence of toluene. The higher concentration in naphthalene precursors leads to higher formation rates of naphthalene and subsequently larger, soot forming PAHs. The more efficient production of soot precursors at lower temperatures explains the earlier soot inception in the presence of toluene as seen in Fig. 5 and 6.

4 Conclusions

A well-established Yale burner was extended by a vapour delivery system to study soot formation during the combustion of more realistic, liquid hydrocarbons. The effect of toluene on the soot particle evolution inside a *n*-heptane flame was characterised by measuring the particle size distribution with a differential mobility spectrometer. The soot samples from the flame centreline were hereby taken with a newly developed quartz probe that is expected to cause less flame disturbance and enhance diluent/sample mixing. The DMS results showed that soot inception starts closer to the burner when the proportion of toluene is increased. This finding is in agreement with the luminescence zone observed in flame photographs and the HAB at which soot starts to deposit on the thermocouple, causing the measured temperature to decrease with time. The earlier soot inception is suggested to be caused by much higher rates of PAH formation in the presence of toluene. This is consistent with simulations using a simple perfectly-stirred reactor model, which showed differences in the rates of one- and two-ring PAH formation by orders of magnitude. The earlier soot inception in the toluene-containing flames increased the time for soot growth prior to oxidation. The resulting larger particles inside the toluene flames required more time to fully oxidise, which led to a slight increase in the luminescent flame height. The experimental particle size distribution measurements inside a vapour-fed co-flow diffusion flame are the first of their kind and can aid the soot simulation community in testing their models.

Acknowledgements

This project is funded by the National Research Foundation (NRF), Prime Minister's Office, Singapore under its Campus for Research Excellence and Technological Enterprise (CREATE) programme.

References

[1] *4th International Sooting Flame (ISF) Workshop*, 2018. URL https://www.adelaide.edu.au/cet/isfworkshop/2018-workshop/.

[2] A. D. Abid, J. Camacho, D. A. Sheen, and H. Wang. Quantitative measurement of soot particle size distribution in premixed flames – The burner-stabilized stagnation flame approach. *Combust. Flame*, 156:1862–1870, 2009. doi:10.1016/j.combustflame.2009.05.010.

[3] R. Alcántara, J. M. Jiménez-Mateos, P. Lavela, and J. L. Tirado. Carbon black: a promising electrode material for sodium-ion batteries. *Electrochem. Commun.*, 3: 639–642, 2001. doi:10.1016/S1388-2481(01)00244-2.

[4] E. J. Barrientos, M. Lapuerta, and A. L. Boehman. Group additivity in soot formation for the example of C-5 oxygenated hydrocarbon fuels. *Combust. Flame*, 160:1484–1498, 2013. doi:10.1016/J.COMBUSTFLAME.2013.02.024.

[5] M. L. Botero, S. Mosbach, J. Akroyd, and M. Kraft. Sooting tendency of surrogates for the aromatic fractions of diesel and gasoline in a wick-fed diffusion flame. *Fuel*, 153:31–39, 2015. doi:10.1016/j.fuel.2015.02.108.

[6] M. L. Botero, S. Mosbach, and M. Kraft. Sooting tendency and particle size distributions of n-heptane/toluene mixtures burned in a wick-fed diffusion flame. *Fuel*, 169:111–119, 2016. doi:10.1016/j.fuel.2015.12.014.

[7] M. L. Botero, N. Eaves, J. A. Dreyer, Y. Sheng, J. Akroyd, W. Yang, and M. Kraft. Experimental and numerical study of the evolution of soot primary particles in a diffusion flame. *Proc. Combust. Inst.*, 2018. doi:10.1016/J.PROCI.2018.06.185.

[8] H. Calcote and D. Manos. Effect of molecular structure on incipient soot formation. *Combust. Flame*, 49:289–304, 1983. doi:10.1016/0010-2180(83)90172-4.

[9] M. Commodo, G. De Falco, A. Bruno, C. Borriello, P. Minutolo, and A. D'Anna. Physicochemical evolution of nascent soot particles in a laminar premixed flame: from nucleation to early growth. *Combust. Flame*, 162:3854–3863, 2015. doi:10.1016/j.combustflame.2015.07.022.

[10] M. Commodo, A. D'Anna, G. De Falco, R. Larciprete, and P. Minutolo. Illuminating the earliest stages of the soot formation by photoemission and Raman spectroscopy. *Combust. Flame*, 181:188–197, 2017. doi:10.1016/j.combustflame.2017.03.020.

[11] M. Conturso, M. Sirignano, and A. D'Anna. Effect of 2,5-dimethylfuran doping on particle size distributions measured in premixed ethylene/air flames. *Proc. Combust. Inst.*, 36:985–992, 2017. doi:10.1016/j.proci.2016.06.048.

[12] A. E. Daca and Ö. L. Gülder. Soot formation characteristics of diffusion flames of methane doped with toluene and n -heptane at elevated pressures. *Proc. Combust. Inst.*, 36:737–744, 2017. doi:10.1016/j.proci.2016.07.046.

[13] D. D. Das, W. J. Cannella, C. S. McEnally, C. J. Mueller, and L. D. Pfefferle. Two-dimensional soot volume fraction measurements in flames doped with large hydrocarbons. *Proc. Combust. Inst.*, 36:871–879, 2017. doi:10.1016/j.proci.2016.06.047.

[14] D. D. Das, C. S. McEnally, T. A. Kwan, J. B. Zimmerman, W. J. Cannella, C. J. Mueller, and L. D. Pfefferle. Sooting tendencies of diesel fuels, jet fuels, and their surrogates in diffusion flames. *Fuel*, 197:445–458, 2017. doi:10.1016/j.fuel.2017.01.099.

[15] D. D. Das, P. C. St. John, C. S. McEnally, S. Kim, and L. D. Pfefferle. Measuring and predicting sooting tendencies of oxygenates, alkanes, alkenes, cycloalkanes, and aromatics on a unified scale. *Combust. Flame*, 190:349–364, 2018. doi:10.1016/J.COMBUSTFLAME.2017.12.005.

[16] G. De Falco, M. Commodo, A. D'Anna, and P. Minutolo. The evolution of soot particles in premixed and diffusion flames by thermophoretic particle densitometry. *Proc. Combust. Inst.*, 36:763–770, 2017. doi:10.1016/j.proci.2016.07.108.

[17] F. N. Egolfopoulos, N. Hansen, Y. Ju, K. Kohse-Höinghaus, C. K. Law, and F. Qi. Advances and challenges in laminar flame experiments and implications for combustion chemistry. *Prog. Energy Combust. Sci.*, 43:36–67, 2014. doi:10.1016/j.pecs.2014.04.004.

[18] V. Gnielinski. *VDI-Wärmeatlas*, page 817. Springer-Verlag Berlin Heidelberg, 2013.

[19] E. Goudeli, A. J. Gröhn, and S. E. Pratsinis. Sampling and dilution of nanoparticles at high temperature. *Aerosol Sci. Technol.*, 50:591–604, 2016. doi:10.1080/02786826.2016.1168922.

[20] Ö. Gustafsson and V. Ramanathan. Convergence on climate warming by black carbon aerosols. *Proc. Natl. Acad. Sci. U.S.A.*, 113:4243–4245, 2016. doi:10.1073/pnas.1603570113.

[21] H. Hepp and K. Siegmann. Mapping of soot particles in a weakly sooting diffusion flame by aerosol techniques. *Combust. Flame*, 115:275–283, 1998. doi:10.1016/S0010-2180(97)00346-5.

[22] J.-C. Huang. Carbon black filled conducting polymers and polymer blends. *Adv. Polym. Technol.*, 21:299–313, 2002. doi:10.1002/adv.10025.

[23] M. Z. Jacobson. Control of fossil-fuel particulate black carbon and organic matter, possibly the most effective method of slowing global warming. *J. Geophys. Res.: Atmos.*, 107:4410, 2002. doi:10.1029/2001JD001376.

[24] M. Kazemimanesh, A. Moallemi, J. S. Olfert, and L. W. Kostiuk. Probe sampling to map and characterize nanoparticles along the axis of a laminar methane jet diffusion flame. *Proc. Combust. Inst.*, 36:881–888, 2017. doi:10.1016/j.proci.2016.06.169.

[25] N. J. Kempema and M. B. Long. Combined optical and TEM investigations for a detailed characterization of soot aggregate properties in a laminar coflow diffusion flame. *Combust. Flame*, 164:373–385, 2016. doi:10.1016/J.COMBUSTFLAME.2015.12.001.

[26] A. Khosousi, F. Liu, S. B. Dworkin, N. A. Eaves, M. J. Thomson, X. He, Y. Dai, Y. Gao, F. Liu, S. Shuai, and J. Wang. Experimental and numerical study of soot formation in laminar coflow diffusion flames of gasoline/ethanol blends. *Combust. Flame*, 162:3925–3933, 2015. doi:10.1016/j.combustflame.2015.07.029.

[27] J. Lelieveld, J. S. Evans, M. Fnais, D. Giannadaki, and A. Pozzer. The contribution of outdoor air pollution sources to premature mortality on a global scale. *Nature*, 525:367–371, 2015. doi:10.1038/nature15371.

[28] Z. Li, L. Qiu, X. Cheng, Y. Li, and H. Wu. The evolution of soot morphology and nanostructure in laminar diffusion flame of surrogate fuels for diesel. *Fuel*, 211: 517–528, 2018. doi:10.1016/j.fuel.2017.09.036.

[29] R. P. Lindstedt and B. B. O. Waldheim. Modeling of soot particle size distributions in premixed stagnation flow flames. *Proc. Combust. Inst.*, 34:1861–1868, 2013. doi:10.1016/j.proci.2012.05.047.

[30] C. McEnally, A. Schaffer, M. Long, L. Pfefferle, M. Smooke, M. Colket, and R. Hall. Computational and experimental study of soot formation in a coflow, laminar ethylene diffusion flame. *Proc. Combust. Inst.*, 27:1497–1505, 1998. doi:10.1016/S0082-0784(98)80557-2.

[31] C. S. McEnally and L. D. Pfefferle. Experimental Assessment of Naphthalene Formation Mechanisms in Non-Premixed Flames. *Combust. Sci. Technol.*, 128: 257–278, 1997. doi:10.1080/00102209708935712.

[32] C. S. McEnally and L. D. Pfefferle. Improved sooting tendency measurements for aromatic hydrocarbons and their implications for naphthalene formation pathways. *Combust. Flame*, 148:210–222, 2007. doi:10.1016/J.COMBUSTFLAME.2006.11.003.

[33] C. S. McEnally and L. D. Pfefferle. Sooting tendencies of non-volatile aromatic hydrocarbons. *Proc. Combust. Inst.*, 32:673–679, 2009. doi:10.1016/J.PROCI.2008.06.197.

[34] C. S. McEnally and L. D. Pfefferle. Sooting Tendencies of Oxygenated Hydrocarbons in Laboratory-Scale Flames. *Environ. Sci. Technol.*, 45:2498–2503, 2011. doi:10.1021/es103733q.

[35] C. S. McEnally, L. D. Pfefferle, B. Atakan, and K. Kohse-Höinghaus. Studies of aromatic hydrocarbon formation mechanisms in flames: Progress towards closing the fuel gap. *Prog. Energy Combust. Sci.*, 32:247–294, 2006. doi:10.1016/j.pecs.2005.11.003.

[36] A. Naseri, A. Veshkini, and M. J. Thomson. Detailed modeling of CO_2 addition effects on the evolution of soot particle size distribution functions in premixed laminar ethylene flames. *Combust. Flame*, 183:75–87, 2017. doi:10.1016/j.combustflame.2017.04.028.

[37] A. Payne and R. Whittaker. Reinforcement of rubber with carbon black. *Compos.*, 1:203–214, 1970. doi:10.1016/0010-4361(70)90005-4.

[38] A. Raj, I. D. C. Prada, A. A. Amer, and S. H. Chung. A reaction mechanism for gasoline surrogate fuels for large polycyclic aromatic hydrocarbons. *Combust. Flame*, 159:500–515, 2012. doi:10.1016/j.combustflame.2011.08.011.

[39] V. Ramanathan and G. Carmichael. Global and regional climate changes due to black carbon. *Nat. Geosci.*, 1:221–227, 2008. doi:10.1038/ngeo156.

[40] C. Saggese, A. Cuoci, A. Frassoldati, S. Ferrario, J. Camacho, H. Wang, and T. Faravelli. Probe effects in soot sampling from a burner-stabilized stagnation flame. *Combust. Flame*, 167:184–197, 2016. doi:10.1016/j.combustflame.2016.02.013.

[41] C. R. Shaddix. Correcting thermocouple measurements for radiation loss: A critical review. In *Proceedings of the 33rd National Heat Transfer Conference, Albuquerque, New Mexico*, pages HTD99–282. American Society of Mechanical Engineers, Albuquerque, NM, USA, 1999.

[42] M. Smooke, M. Long, B. Connelly, M. Colket, and R. Hall. Soot formation in laminar diffusion flames. *Combust. Flame*, 143:613–628, 2005. doi:10.1016/J.COMBUSTFLAME.2005.08.028.

[43] Y. R. Tan, M. L. Botero, Y. Sheng, J. A. H. Dreyer, R. Xu, W. Yang, and M. Kraft. Sooting characteristics of polyoxymethylene dimethyl ether blends with diesel in a diffusion flame. *Fuel*, 224:499–506, 2018. doi:10.1016/j.fuel.2018.03.051.

[44] Q. Tang, B. Ge, Q. Ni, B. Nie, and X. You. Soot formation characteristics of n-heptane/toluene mixtures in laminar premixed burner-stabilized stagnation flames. *Combust. Flame*, 187:239–246, 2018. doi:10.1016/j.combustflame.2017.08.022.

[45] A. Veshkini, N. A. Eaves, S. B. Dworkin, and M. J. Thomson. Application of PAH-condensation reversibility in modeling soot growth in laminar premixed and nonpremixed flames. *Combust. Flame*, 167:335–352, 2016. doi:10.1016/j.combustflame.2016.02.024.

[46] E. K. Yapp, D. Chen, J. Akroyd, S. Mosbach, M. Kraft, J. Camacho, and H. Wang. Numerical simulation and parametric sensitivity study of particle size distributions in a burner-stabilised stagnation flame. *Combust. Flame*, 162:2569–2581, 2015. doi:10.1016/j.combustflame.2015.03.006.

[47] E. K. Y. Yapp, R. I. A. Patterson, J. Akroyd, S. Mosbach, E. M. Adkins, J. Houston Miller, and M. Kraft. Numerical simulation and parametric sensitivity study of optical band gap in a laminar co-flow ethylene diffusion flame. *Combustion and Flame*, 167:320–334, 2016. doi:10.1016/j.combustflame.2016.01.033.

[48] K.-S. Yun, B.-R. Kim, E. Noh, H.-J. Jung, H.-J. Oh, W.-S. Kang, S.-C. Jung, S.-T. Myung, and S.-J. Kim. Microstructural Effect of Carbon Blacks for the Application in Lithium Ion Batteries. *Jpn. J. Appl. Phys.*, 52:11NM01, 2013. doi:10.7567/JJAP.52.11NM01.

[49] T. Zhang, L. Zhao, and M. J. Thomson. Effects of n-propylbenzene addition to n-dodecane on soot formation and aggregate structure in a laminar coflow diffusion flame. *Proc. Combust. Inst.*, 36:1339–1347, 2017. doi:10.1016/j.proci.2016.05.026.

[50] B. Zhao, Z. Yang, J. Wang, M. V. Johnston, and H. Wang. Analysis of Soot Nanoparticles in a Laminar Premixed Ethylene Flame by Scanning Mobility Particle Sizer. *Aerosol Sci. Technol.*, 37:611–620, 2003. doi:10.1080/02786820300908.

Supporting information

These supporting information provide additional figures and tables to substantiate the results and discussions presented in the main article. In addition, all the raw data presented in Fig. 5 of the main manuscript are provided in Tables S2–S5 to facilitate the validation of numerical soot models and comparison to other experimental studies. The values are corrected for dilution and the temperature at the sample tip but not sample losses in the lines. The numbers are in $dN/dlogD_p$ (cm^{-3}); the absolute particle number density can be obtained by summation over all particle sizes and dividing by 16 in accordance with the DMS500 manual. A technical drawing of the quartz probe developed to take the soot samples from within the flame is shown on the last page.

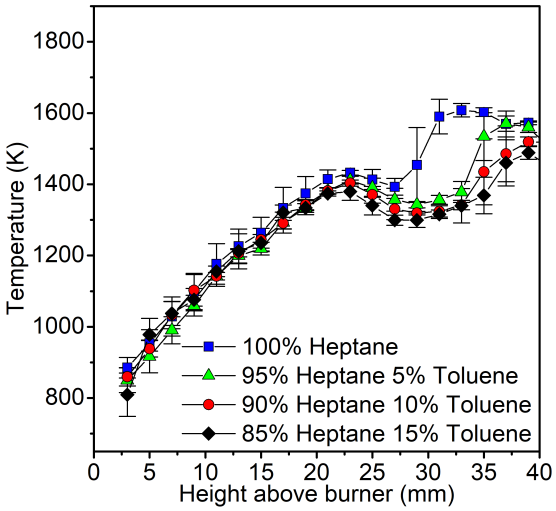

Figure S1: *Uncorrected flame temperatures as measured by fast insertion of a S-type thermocouple.*

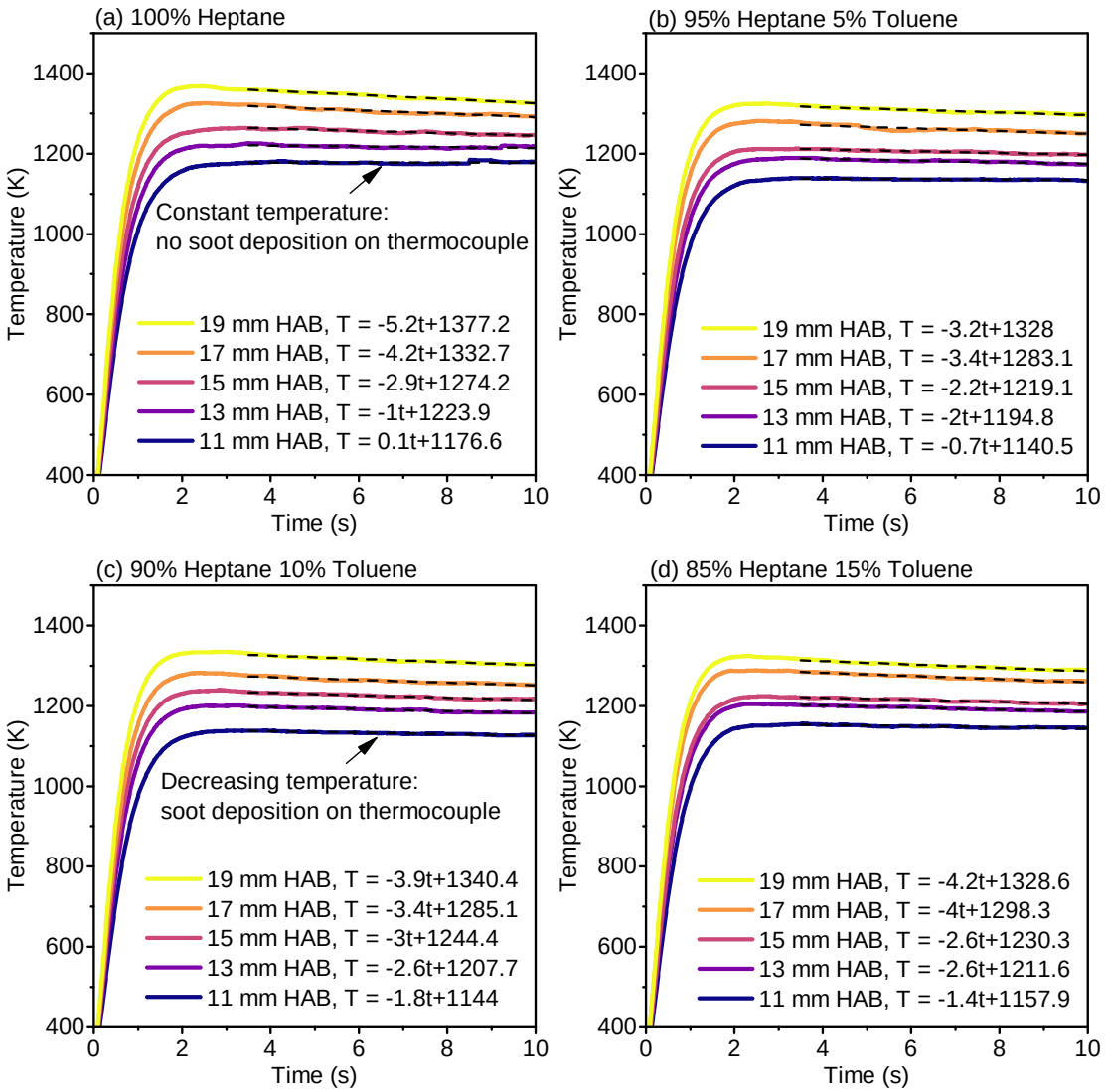

Figure S2: *Time resolved flame temperature measurements at different HAB. The dashed lines are linear regressions between 3.5-10 s and the resulting equations are shown in the figure legends.*

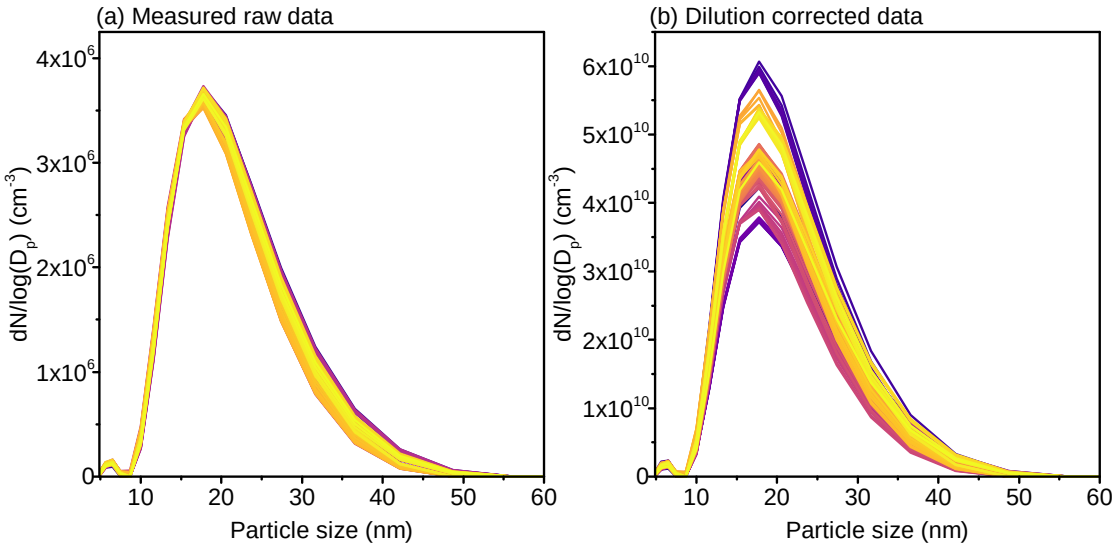

Figure S3: *Particle size distribution in the centre of a heptane flame at 22 mm HAB. The as-measured data shown in (a) was corrected for N2 dilution in (b).*

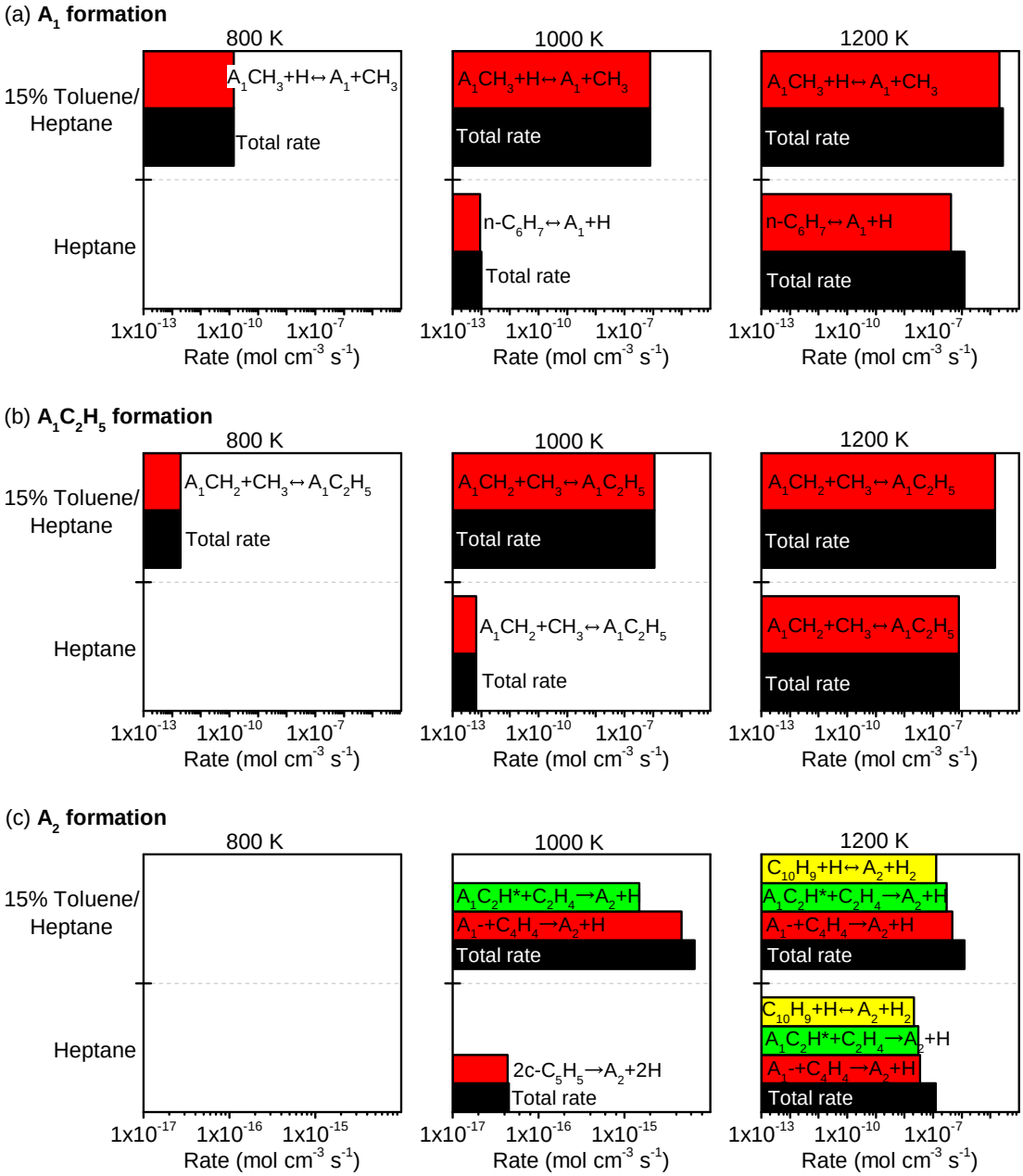

Figure S4: *Rates of (a) benzene (A_1), (b) ethylbenzene ($A_1C_2H_5$), and (c) naphthalene (A_2) formation from pure heptane and 15 % toluene/heptane at 800 K, 1000 K, and 1200 K. Also shown are the main reactions contributing to the overall rate of formation.*

Table S1: *Reaction rates and main reaction routes for the consumption of toluene (A_1CH_3) and benzyl radical (A_1CH_2) and the formation of benzene (A_1), methyl radical (CH_3), phenyl radical (A_1-), phenylacetylene (A_1C_2H), ethylbenzene ($A_1C_2H_5$), and naphthalene (A_2). Details on the mechanism and notation can be found in [38]. The relative contribution of the respective route to the overall reaction rate is given in brackets.*

		800 K		1000 K		1200 K	
		Hep.	15% Tol./Hep.	Hep.	15% Tol./Hep.	Hep.	15% Tol./Hep.
Rate toluene ($mol \cdot cm^{-3} \cdot s^{-1}$)		$2.76 \cdot 10^{-28}$	$2.38 \cdot 10^{-10}$	$6.98 \cdot 10^{-18}$	$1.97 \cdot 10^{-6}$	$1.86 \cdot 10^{-7}$	$3.81 \cdot 10^{-5}$
Route toluene consumption	1a	N/A	$A_1CH_3+H \leftrightarrow A_1+CH_3$ (0.599)	$A_1CH_3+CH_2 \leftrightarrow A_1C_2H_3+H_2$ (0.999)	$A_1CH_3+CH_3 \leftrightarrow A_1CH_2+CH_4$ (0.520)	$A_1CH_3+CH_3 \leftrightarrow A_1CH_2+CH_4$ (0.329)	$A_1CH_3+H \leftrightarrow A_1+CH_3$ (0.541)
	1b		$A_1CH_3+CH_3 \leftrightarrow A_1CH_2+CH_4$ (0.353)		$A_1CH_3+H \leftrightarrow A_1+CH_3$ (0.401)	$A_1CH_3+H \leftrightarrow A_1+CH_3$ (0.269)	$A_1CH_3+H \leftrightarrow A_1CH_2+H_2$ (0.216)
	1c		$A_1CH_3+H \leftrightarrow A_1CH_2+H_2$ (0.048)		$A_1CH_3+H \leftrightarrow A_1CH_2+H_2$ (0.075)	$A_1CH_3+H \leftrightarrow A_1CH_2+H_2$ (0.239)	$A_1CH_3+CH_3 \leftrightarrow A_1CH_2+CH_4$ (0.214)
	1d					$A_1CH_3+C_3H_2 \leftrightarrow C_{10}H_{10}$ (0.158)	
Rate A_1 ($mol \cdot cm^{-3} \cdot s^{-1}$)		$1.29 \cdot 10^{-26}$	$1.43 \cdot 10^{-10}$	$1.01 \cdot 10^{-12}$	$8.01 \cdot 10^{-7}$	$1.24 \cdot 10^{-6}$	$2.69 \cdot 10^{-5}$
	2a	N/A	$A_1CH_3+H \leftrightarrow A_1+CH_3$ (1.0)	*n*-$C_6H_7 \leftrightarrow A_1+H$ (0.903)	$A_1CH_3+H \leftrightarrow A_1+CH_3$ (0.987)	*n*-$C_6H_7 \leftrightarrow A_1+H$ (0.335)	$A_1CH_3+H \leftrightarrow A_1+CH_3$ (0.765)
Route A_1 formation	2b					*l*-$C_6H_6+H \leftrightarrow A_1+H$(0.176)	A_1-$+C_2H_4 \leftrightarrow A_1+C_2H_3$ (0.107)
	2c				A_1-$+C_2H_4 \leftrightarrow A_1+C_2H_3$ (0.146)	$A_1C_2H_5+H \leftrightarrow A_1+C_2H_5$(0.075)	
	2d				$A_1C_2H_5+H \leftrightarrow A_1+C_2H_5$(0.093)		
Rate CH_3 ($mol \cdot cm^{-3} \cdot s^{-1}$)		$3.95 \cdot 10^{-8}$	$7.19 \cdot 10^{-9}$	$5.20 \cdot 10^{-5}$	$1.99 \cdot 10^{-5}$	$2.43 \cdot 10^{-4}$	$2.31 \cdot 10^{-4}$
Route CH_3 formation	3a	*n*-$C_3H_7 \leftrightarrow CH_3+C_2H_4$ (1.0)	$A_1CH_3+H_2 \leftrightarrow A_1+CH_3$ (0.02)	*n*-$C_3H_7 \leftrightarrow CH_3+C_2H_4$ (1.0)	*n*-$C_3H_7 \leftrightarrow CH_3+C_2H_4$ (0.960)	*n*-$C_3H_7 \leftrightarrow CH_3+C_2H_4$ (0.888)	*n*-$C_3H_7 \leftrightarrow CH_3+C_2H_4$ (0.860)
	3b		*n*-$C_3H_7 \leftrightarrow CH_3+C_2H_4$ (0.98)			$2CH_3 \leftrightarrow H+C_2H_5$ (0.035)	$A_1CH_3+H \leftrightarrow A_1+CH_3$ (0.089)
Rate A_1- ($mol \cdot cm^{-3} \cdot s^{-1}$)		$3.55 \cdot 10^{-23}$	$1.69 \cdot 10^{-16}$	$1.91 \cdot 10^{-14}$	$9.63 \cdot 10^{-9}$	$5.59 \cdot 10^{-7}$	$1.93 \cdot 10^{-5}$
Route A_1- formation	4a	N/A	$A_1+CH_3 \leftrightarrow A_1$-$+CH_4$ (0.675)	$A_1+CH_3 \leftrightarrow A_1$-$+CH_4$ (0.602)	$A_1+CH_3 \leftrightarrow A_1$-$+CH_4$ (0.559)	A_1-$+C_2H_6 \leftrightarrow A_1C_2H_5+H$ (0.532)	$A_1+CH_3 \rightarrow A_1$-$+CH_4$ (0.548)
	4b		$A_1CH_3+H \leftrightarrow A_1$-$+CH_4$ (0.308)	A_1-$+C_2H_6 \leftrightarrow A_1C_2H_5+H$ (0.376)	A_1-$+C_2H_6 \leftrightarrow A_1C_2H_5+H$ (0.441)	$A_1+CH_3 \leftrightarrow A_1$-$+CH_4$ (0.379)	$A_1C_2H_5+H \leftrightarrow A_1$-$+C_2H_6$ (0.437)
Rate A_1CH_2 ($mol \cdot cm^{-3} \cdot s^{-1}$)		$2.48 \cdot 10^{-25}$	$9.55 \cdot 10^{-11}$	$6.72 \cdot 10^{-13}$	$1.18 \cdot 10^{-6}$	$1.11 \cdot 10^{-6}$	$1.81 \cdot 10^{-5}$
Route A_1CH_2 formation	5a	N/A	$A_1CH_3+CH_3 \leftrightarrow A_1CH_2+CH_4$ (0.881)	$A_1CH_2 \leftrightarrow c$-$C_5H_5+C_2H_2$ (1.000)	$A_1CH_3+CH_3 \leftrightarrow A_1CH_2+CH_4$ (0.868)	$A_1CH_2 \leftrightarrow c$-$C_5H_5+C_2H_2$ (0.889)	$A_1CH_3+H \leftrightarrow A_1CH_2+H_2$ (0.454)
	5b		$A_1CH_3+H \leftrightarrow A_1CH_2+H_2$ (0.119)		$A_1CH_3+H \leftrightarrow A_1CH_2+H_2$ (0.124)	$A_1CH_3+CH_3 \leftrightarrow A_1CH_2+CH_4$ (0.055)	$A_1CH_3+CH_3 \leftrightarrow A_1CH_2+CH_4$ (0.450)
Rate A_1CH_2 ($mol \cdot cm^{-3} \cdot s^{-1}$)		$4.28 \cdot 10^{-28}$	$1.97 \cdot 10^{-12}$	$6.60 \cdot 10^{-13}$	$1.13 \cdot 10^{-6}$	$1.11 \cdot 10^{-6}$	$1.80 \cdot 10^{-5}$
Route A_1CH_2 consumption	6a	N/A	$A_1CH_2+CH_3 \leftrightarrow A_1C_2H_5$ (0.996)	$A_1CH_2+CH_3 \leftrightarrow A_1C_2H_5$ (0.980)	$A_1CH_2+CH_3 \leftrightarrow A_1C_2H_5$ (0.982)	$A_1CH_2+CH_3 \leftrightarrow A_1C_2H_5$ (0.701)	$A_1CH_2+CH_3 \leftrightarrow A_1C_2H_5$ (0.792)
	6b					$A_1CH_3 \leftrightarrow A_1CH_2+H_2$ (0.164)	$A_1CH_3 \leftrightarrow A_1CH_2+H_2$ (0.177)
	6c					A_1CH_3+c-$C_5H_5 \leftrightarrow A_1CH_2+c$-$C_5H_6$ (0.106)	$A_1CH_2+C_3H_3 \leftrightarrow C_{10}H_{10}$ (0.015)
Rate A_1C_2H ($mol \cdot cm^{-3} \cdot s^{-1}$)		$2.28 \cdot 10^{-29}$	$5.96 \cdot 10^{-26}$	$4.71 \cdot 10^{-17}$	$3.00 \cdot 10^{-12}$	$3.15 \cdot 10^{-7}$	$3.46 \cdot 10^{-6}$
Route A_1C_2H formation	7a	N/A	N/A	$A_1C_2H+H \leftrightarrow A_1C_2H2$ (0.966)	$A_1C_2H+H \leftrightarrow A_1C_2H2$ (0.954)	$A_1C_2H+H \leftrightarrow A_1C_2H2$ (0.853)	$A_1C_2H+H \leftrightarrow A_1C_2H2$ (0.848)
	7b				$A_1+C_2H_2 \leftrightarrow A_1C_2H+H$ (0.046)	$A_1+C_2H_2 \leftrightarrow A_1C_2H+H$ (0.098)	$A_1+C_2H_2 \leftrightarrow A_1C_2H+H$ (0.029)
Rate $A_1C_2H_5$ ($mol \cdot cm^{-3} \cdot s^{-1}$)		$7.62 \cdot 10^{-29}$	$1.97 \cdot 10^{-12}$	$6.55 \cdot 10^{-13}$	$1.12 \cdot 10^{-6}$	$7.94 \cdot 10^{-7}$	$1.46 \cdot 10^{-5}$
Route $A_1C_2H_5$ formation	8a	N/A	$A_1CH_2+CH_3 \leftrightarrow A_1C_2H_5$ (0.996)	$A_1CH_2+CH_3 \leftrightarrow A_1C_2H_5$ (0.988)	$A_1CH_2+CH_3 \leftrightarrow A_1C_2H_5$ (0.988)	$A_1CH_2+CH_3 \leftrightarrow A_1C_2H_5$ (0.979)	$A_1CH_2+CH_3 \leftrightarrow A_1C_2H_5$ (0.979)
Rate A_2 ($mol \cdot cm^{-3} \cdot s^{-1}$)		$8.83 \cdot 10^{-32}$	$1.24 \cdot 10^{-26}$	$4.5 \cdot 10^{-17}$	$6.56 \cdot 10^{-15}$	$1.23 \cdot 10^{-7}$	$1.23 \cdot 10^{-6}$
Route A_2 formation	9a	N/A	N/A	2*c*-$C_5H_5 \rightarrow A_2+2H$ (0.974)	A_1-$+C_4H_4 \rightarrow A_2+H$ (0.701)	A_1-$+C_4H_4 \rightarrow A_2+H$ (0.286)	A_1-$+C_4H_4 \rightarrow A_2+H$ (0.381)
	9b				$A_1C_2H^*+C_2H_4 \rightarrow A_2+H$ (0.227)	$A_1C_2H^*+C_2H_4 \rightarrow A_2+H$ (0.250)	$A_1C_2H^*+C_2H_4 \rightarrow A_2+H$ (0.243)
	9c				$A_1C_2H+C_2H_3 \rightarrow A_2+H$ (0.054)	$C_{10}H_9+H \leftrightarrow A_2+H_2$ (0.171)	$C_{10}H_9+H \leftrightarrow A_2+H_2$ (0.104)

Table S2: *Averaged measured soot particle size distributions along the centreline of the heptane flame in dN/dlogD_p (cm^{-3}).*

	HAB (mm)										
D_p (nm)	10	11	12	13	14	15	16	17	18	19	20
4.87	9.1044E+07	9.4909E+07	9.3828E+07	2.4625E+08	4.5570E+08	6.3897E+08	6.6337E+08	6.5728E+08	5.1116E+08	2.2908E+08	2.2965E+08
5.62	1.0898E+08	1.1172E+08	1.1019E+08	3.6486E+08	7.8661E+08	1.6244E+09	1.9674E+09	1.8228E+09	1.5938E+09	6.9696E+08	4.6650E+08
6.49	9.5710E+07	9.1974E+07	8.8019E+07	3.3408E+08	8.2806E+08	2.3943E+09	3.4800E+09	3.6745E+09	3.4815E+09	2.2356E+09	1.8336E+09
7.5	8.3543E+07	7.9767E+07	6.7290E+07	2.3366E+08	6.1851E+08	2.4601E+09	4.6155E+09	6.1154E+09	7.0765E+09	6.7517E+09	6.6202E+09
8.66	6.1847E+07	5.7982E+07	4.1010E+07	1.1630E+08	3.1289E+08	1.8677E+09	4.9792E+09	8.3055E+09	1.1359E+10	1.3110E+10	1.4280E+10
10	5.9074E+07	5.4586E+07	3.5342E+07	4.8477E+07	9.1200E+07	1.0573E+09	4.4580E+09	9.0942E+09	1.4342E+10	1.8607E+10	2.2386E+10
11.55	6.4747E+07	5.9947E+07	3.6083E+07	3.2057E+07	1.7910E+07	4.3711E+08	3.2431E+09	7.9300E+09	1.4589E+10	2.0937E+10	2.8203E+10
13.34	6.2672E+07	5.8496E+07	2.8987E+07	2.7950E+07	1.2058E+07	1.2160E+08	1.8006E+09	5.4127E+09	1.2301E+10	1.9695E+10	3.0070E+10
15.4	6.0673E+07	5.6862E+07	2.4585E+07	2.8008E+07	1.3251E+07	2.5181E+07	6.5160E+08	2.7111E+09	8.6874E+09	1.5834E+10	2.7548E+10
17.78	5.6324E+07	5.1658E+07	2.1103E+07	2.7250E+07	1.5483E+07	9.0183E+06	8.9182E+07	8.7606E+08	5.1144E+09	1.0881E+10	2.1487E+10
20.54	4.7428E+07	4.0904E+07	1.5028E+07	2.2924E+07	1.3786E+07	9.9161E+06	4.8499E+06	1.0575E+08	2.4051E+09	6.2571E+09	1.4049E+10
23.71	3.8428E+07	3.1160E+07	1.1014E+07	1.8588E+07	1.1390E+07	9.9394E+06	3.7241E+06	5.6478E+06	7.8135E+08	2.9281E+09	7.5930E+09
27.38	3.0936E+07	2.4876E+07	9.0827E+06	1.4959E+07	9.2114E+06	9.0408E+06	3.3806E+06	4.1035E+06	1.2341E+08	9.4620E+08	3.2282E+09
31.62	2.6386E+07	2.1977E+07	8.8008E+06	1.2748E+07	7.8862E+06	8.2109E+06	5.0652E+06	3.8501E+06	2.4989E+06	9.9617E+07	8.7922E+08
36.52	2.3805E+07	2.0911E+07	8.8951E+06	1.1210E+07	7.2982E+06	7.5953E+06	7.8930E+06	4.5124E+06	4.4513E+06	1.2434E+06	4.6252E+07
42.17	2.2298E+07	2.0650E+07	9.2600E+06	1.0329E+07	7.3655E+06	7.1477E+06	1.0127E+07	5.9437E+06	5.5526E+06	3.5466E+06	7.9739E+06
48.7	2.1594E+07	2.0310E+07	9.6503E+06	9.8706E+06	7.5792E+06	6.7240E+06	1.0532E+07	7.2130E+06	5.6805E+06	5.4414E+06	9.1478E+06
56.23	2.0983E+07	1.9577E+07	9.8904E+06	1.0028E+07	7.5996E+06	6.5062E+06	9.8212E+06	7.4958E+06	6.2354E+06	5.9066E+06	1.0196E+07
64.94	2.0035E+07	1.8457E+07	9.6202E+06	1.0163E+07	7.2093E+06	6.3573E+06	8.7613E+06	6.6537E+06	7.2029E+06	5.2436E+06	1.0753E+07
74.99	1.8390E+07	1.6534E+07	8.6215E+06	9.8919E+06	6.5417E+06	5.9706E+06	7.6799E+06	5.2876E+06	7.6675E+06	4.8510E+06	9.9341E+06
86.6	1.6237E+07	1.4228E+07	7.3182E+06	8.9374E+06	5.5631E+06	5.2770E+06	6.7572E+06	4.4569E+06	6.9582E+06	4.8947E+06	8.4760E+06
100	1.3896E+07	1.1925E+07	5.9704E+06	7.4852E+06	4.6222E+06	4.4905E+06	5.9243E+06	4.0467E+06	5.3590E+06	4.2084E+06	6.9780E+06
115.48	1.1577E+07	9.8364E+06	4.7768E+06	5.9000E+06	3.8644E+06	3.6380E+06	4.9887E+06	3.8679E+06	3.9270E+06	2.9010E+06	5.8322E+06
133.35	9.4308E+06	7.9176E+06	3.7688E+06	4.4995E+06	3.1953E+06	2.8504E+06	4.0276E+06	3.4445E+06	3.2916E+06	2.3879E+06	4.7705E+06
153.99	7.3875E+06	6.1812E+06	2.9675E+06	3.4219E+06	2.5069E+06	2.2316E+06	3.1650E+06	2.6815E+06	2.8093E+06	2.3845E+06	3.9778E+06
177.83	5.5109E+06	4.6610E+06	2.3618E+06	2.6434E+06	1.8474E+06	1.8051E+06	2.4436E+06	1.8859E+06	2.3677E+06	2.4719E+06	3.2773E+06
205.35	4.0886E+06	3.5073E+06	1.8587E+06	2.0635E+06	1.3214E+06	1.4520E+06	1.8796E+06	1.3184E+06	1.8837E+06	2.2839E+06	2.7184E+06
237.14	3.2284E+06	2.7100E+06	1.4076E+06	1.6169E+06	9.7375E+05	1.1144E+06	1.5005E+06	9.7032E+05	1.4416E+06	1.8658E+06	2.1623E+06
273.84	2.7739E+06	2.1457E+06	1.0741E+06	1.2833E+06	7.6851E+05	8.2912E+05	1.2404E+06	7.5761E+05	1.0838E+06	1.3957E+06	1.6525E+06
316.23	2.4842E+06	1.7427E+06	8.3851E+05	1.0238E+06	6.3247E+05	6.1896E+05	1.0329E+06	6.1561E+05	8.8893E+05	1.0235E+06	1.2364E+06
365.17	2.1677E+06	1.4112E+06	6.7706E+05	8.2356E+05	5.3274E+05	4.8118E+05	8.4550E+05	5.1907E+05	7.7255E+05	7.8824E+05	9.3883E+05
421.7	1.7870E+06	1.1294E+06	5.7282E+05	6.5445E+05	4.4262E+05	3.8397E+05	6.7214E+05	4.4134E+05	6.6024E+05	6.4004E+05	7.3234E+05
486.97	1.3888E+06	8.8331E+05	5.0667E+05	5.0444E+05	3.5528E+05	3.1243E+05	5.1650E+05	3.7054E+05	5.5191E+05	5.2121E+05	5.8779E+05
562.34	1.0515E+06	6.7105E+05	4.5500E+05	3.8862E+05	2.8856E+05	2.7332E+05	3.8592E+05	3.0865E+05	4.4744E+05	4.1499E+05	4.6069E+05
649.38	8.4648E+05	5.2221E+05	4.2676E+05	3.1569E+05	2.4378E+05	2.5254E+05	3.0527E+05	2.6335E+05	3.5180E+05	3.3449E+05	3.7254E+05
749.89	7.8635E+05	4.4249E+05	4.1130E+05	2.8069E+05	2.2131E+05	2.4140E+05	2.6983E+05	2.3813E+05	2.8876E+05	2.9256E+05	3.4260E+05
865.96	8.2392E+05	4.1870E+05	3.9556E+05	2.7130E+05	2.0732E+05	2.2229E+05	2.5988E+05	2.2752E+05	2.5704E+05	2.8159E+05	3.5837E+05
1000	9.2829E+05	4.5874E+05	3.8330E+05	2.7878E+05	1.9057E+05	1.9757E+05	2.5547E+05	2.1629E+05	2.5392E+05	2.8385E+05	4.1581E+05

	HAB (mm)										
dN/dlogD_p (nm)	21	22	23	24	25	26	27	28	29	30	31
4.87	2.5255E+08	3.4230E+08	3.2966E+08	2.3339E+08	1.6321E+08	1.5076E+08	4.5997E+07	8.6046E+07	8.0102E+07	3.9431E+08	3.8587E+07
5.62	4.7265E+08	1.0074E+09	1.2331E+09	9.2682E+08	7.1089E+08	6.2079E+08	1.0836E+08	1.7979E+08	1.3043E+08	6.0054E+08	4.8292E+07
6.49	8.1064E+08	1.3007E+09	1.4701E+09	1.1355E+09	9.2826E+08	8.4976E+08	1.6852E+08	2.3016E+08	1.3353E+08	5.2619E+08	4.8881E+07
7.5	3.4251E+09	1.3567E+09	3.8825E+08	1.9491E+08	1.3268E+08	1.3440E+08	8.0755E+07	6.6765E+07	3.4234E+07	2.4798E+08	3.1877E+07
8.66	9.0658E+09	3.4996E+09	3.4026E+08	3.4847E+06	2.0452E+05	0.0000E+00	0.0000E+00	0.0000E+00	0.0000E+00	0.0000E+00	0.0000E+00
10	1.7493E+10	1.0604E+10	4.2288E+09	2.3484E+09	1.1924E+09	3.2583E+08	6.2176E+06	0.0000E+00	0.0000E+00	6.9865E+05	0.0000E+00
11.55	2.6964E+10	2.3235E+10	1.5231E+10	1.1706E+10	9.7618E+09	8.5199E+09	1.9457E+09	2.5657E+09	1.0906E+09	6.2608E+08	6.2517E+07
13.34	3.4386E+10	3.7196E+10	3.0323E+10	2.6427E+10	2.4305E+10	2.3572E+10	6.4487E+09	7.9888E+09	3.6612E+09	2.4976E+09	1.0129E+09
15.4	3.6747E+10	4.6507E+10	4.3680E+10	4.1339E+10	4.0244E+10	4.1413E+10	1.2966E+10	1.4550E+10	5.9802E+09	4.0650E+09	2.0190E+09
17.78	3.2848E+10	4.7138E+10	5.0297E+10	5.1205E+10	5.2523E+10	5.7009E+10	2.0404E+10	2.0387E+10	6.4858E+09	3.8231E+09	2.0914E+09
20.54	2.4715E+10	4.0142E+10	4.9261E+10	5.4031E+10	5.8501E+10	6.6945E+10	2.7757E+10	2.5239E+10	5.7876E+09	2.1205E+09	1.1857E+09
23.71	1.5847E+10	2.9554E+10	4.2604E+10	5.0548E+10	5.7875E+10	6.9800E+10	3.4193E+10	2.9837E+10	5.8495E+09	6.8401E+08	0.0000E+00
27.38	8.5956E+09	1.8920E+10	3.3097E+10	4.2790E+10	5.1989E+10	6.6178E+10	3.8884E+10	3.4436E+10	8.1782E+09	1.4579E+09	0.0000E+00
31.62	3.7306E+09	1.0316E+10	2.3184E+10	3.3083E+10	4.2932E+10	5.7915E+10	4.1134E+10	3.8625E+10	1.3299E+10	5.6535E+09	1.3663E+09
36.52	1.2306E+09	4.6551E+09	1.4548E+10	2.3301E+10	3.2605E+10	4.6935E+10	4.0773E+10	4.1810E+10	2.0444E+10	1.3139E+10	5.5288E+09
42.17	1.9755E+08	1.7478E+09	8.0835E+09	1.4810E+10	2.2649E+10	3.5174E+10	3.7871E+10	4.3266E+10	2.8266E+10	2.2877E+10	1.2347E+10
48.7	1.5413E+07	4.7256E+08	3.9790E+09	8.4298E+09	1.4322E+10	2.4356E+10	3.2700E+10	4.2262E+10	3.5099E+10	3.3242E+10	2.1074E+10
56.23	3.2842E+06	6.3203E+07	1.7934E+09	4.2773E+09	8.1952E+09	1.5540E+10	2.6011E+10	3.8339E+10	3.8718E+10	4.1204E+10	2.9361E+10
64.94	7.7489E+06	3.0855E+06	7.4655E+08	1.9697E+09	4.2298E+09	9.1013E+09	1.8821E+10	3.1810E+10	3.7801E+10	4.4236E+10	3.4665E+10
74.99	1.2196E+07	1.2623E+06	2.4583E+08	8.5597E+08	1.9762E+09	4.8619E+09	1.2174E+10	2.3654E+10	3.2280E+10	4.1128E+10	3.5157E+10
86.6	1.3590E+07	6.0680E+06	5.8472E+07	3.1901E+08	8.1584E+08	2.3388E+09	6.8597E+09	1.5353E+10	2.3682E+10	3.2814E+10	3.0622E+10
100	1.1594E+07	1.1871E+07	1.3987E+07	9.2583E+07	2.7559E+08	9.6333E+08	3.2249E+09	8.3536E+09	1.4475E+10	2.1995E+10	2.2617E+10
115.48	8.0114E+06	1.3083E+07	1.6556E+07	2.6605E+07	7.9740E+07	3.2938E+08	1.1597E+09	3.5217E+09	6.9382E+09	1.1851E+10	1.3742E+10
133.35	5.3188E+06	9.9696E+06	1.9981E+07	1.5968E+07	2.7115E+07	9.3772E+07	2.5130E+08	9.3212E+08	2.2589E+09	4.6516E+09	6.4288E+09
153.99	4.0733E+06	5.7934E+06	1.5160E+07	1.4999E+07	1.8603E+07	3.3212E+07	2.9893E+06	1.7112E+07	2.8088E+08	9.8744E+08	1.9573E+09
177.83	3.7633E+06	3.3093E+06	7.2043E+06	1.0996E+07	1.4864E+07	1.7899E+07	1.0580E+07	9.6162E+05	0.0000E+00	0.0000E+00	1.6298E+08
205.35	3.5297E+06	2.6435E+06	2.2895E+06	5.5446E+06	9.8523E+06	1.3884E+07	2.2439E+07	6.5440E+06	0.0000E+00	0.0000E+00	0.0000E+00
237.14	3.0911E+06	2.8615E+06	1.2725E+06	2.0995E+06	5.3055E+06	1.1649E+07	2.5127E+07	1.4845E+07	7.0159E+04	0.0000E+00	0.0000E+00
273.84	2.5237E+06	2.9732E+06	1.7413E+06	9.8634E+05	1.7812E+06	7.2808E+06	1.7321E+07	1.4542E+07	5.0947E+05	5.0471E+06	0.0000E+00
316.23	1.9871E+06	2.7349E+06	2.0855E+06	1.3316E+06	5.2640E+05	2.8740E+06	8.3174E+06	1.0567E+07	1.6682E+06	1.1615E+07	0.0000E+00
365.17	1.5347E+06	2.2121E+06	2.0380E+06	1.5220E+06	5.9573E+05	6.8734E+05	2.6804E+06	5.9849E+06	2.9152E+06	1.5771E+07	0.0000E+00
421.7	1.1451E+06	1.5850E+06	1.6535E+06	1.4085E+06	6.5219E+05	4.3300E+05	6.8294E+05	2.5473E+06	2.8282E+06	1.3638E+07	0.0000E+00
486.97	8.2294E+05	1.0171E+06	1.1294E+06	1.1459E+06	6.0716E+05	4.6925E+05	1.0085E+04	5.1669E+05	1.1749E+06	6.6831E+06	2.3325E+04
562.34	5.6118E+05	5.9392E+05	6.7937E+05	9.0681E+05	5.1787E+05	4.2539E+05	1.9460E+04	0.0000E+00	0.0000E+00	1.9139E+03	3.4168E+04
649.38	3.8666E+05	3.4690E+05	3.9309E+05	7.6567E+05	4.3435E+05	3.6532E+05	5.2193E+04	1.5889E+04	0.0000E+00	0.0000E+00	0.0000E+00
749.89	3.2276E+05	2.8476E+05	3.2167E+05	7.2019E+05	3.8275E+05	3.2368E+05	1.0986E+05	1.1080E+05	0.0000E+00	0.0000E+00	0.0000E+00
865.96	3.6656E+05	3.6615E+05	3.7556E+05	7.2786E+05	3.7057E+05	3.0173E+05	1.8869E+05	2.5228E+05	0.0000E+00	0.0000E+00	0.0000E+00
1000	5.0929E+05	5.6873E+05	5.4179E+05	7.7281E+05	3.7408E+05	2.9500E+05	2.3966E+05	4.1085E+05	3.5649E+05	2.3422E+06	0.0000E+00

	HAB (mm)								
D_p (nm)	32	33	34	35	36	37	38	39	40
4.87	4.9644E+07	3.3701E+07	3.2681E+07	9.0203E+07	3.5729E+07	2.2481E+07	3.8238E+07	2.0300E+08	6.5385E+07
5.62	6.2019E+07	4.1439E+07	3.8983E+07	1.2819E+08	4.4983E+07	2.8470E+07	5.4205E+07	2.9661E+08	9.3117E+07
6.49	6.2182E+07	4.5527E+07	4.2351E+07	1.1857E+08	4.8239E+07	2.8994E+07	6.6654E+07	3.3483E+08	1.3945E+08
7.5	4.3445E+07	3.4737E+07	3.1951E+07	6.8653E+07	3.5140E+07	2.0853E+07	4.4847E+07	2.4018E+08	1.9769E+08
8.66	0.0000E+00	0.0000E+00	3.3579E+05	2.9510E+06	8.6929E+05	3.8403E+05	2.1943E+05	1.2237E+08	3.4292E+08
10	0.0000E+00	0.0000E+00	0.0000E+00	5.4152E+04	0.0000E+00	0.0000E+00	1.1844E+06	3.8597E+08	7.4293E+08
11.55	5.0071E+06	1.0469E+06	9.7945E+05	2.6053E+07	5.1100E+06	1.3646E+07	1.9174E+08	1.5903E+09	1.4238E+09
13.34	6.4250E+08	4.1948E+08	3.1441E+08	3.7093E+08	3.2162E+08	3.7200E+08	7.8039E+08	3.3722E+09	2.2420E+09
15.4	1.6448E+09	1.2618E+09	1.0108E+09	1.0491E+09	9.4722E+08	9.5094E+08	1.3693E+09	4.8461E+09	2.9837E+09
17.78	2.2644E+09	1.9564E+09	1.6378E+09	1.6381E+09	1.4584E+09	1.2681E+09	1.5148E+09	5.4002E+09	3.4892E+09
20.54	1.9984E+09	1.9271E+09	1.6709E+09	1.6462E+09	1.4338E+09	1.0648E+09	1.2057E+09	5.3989E+09	3.7478E+09
23.71	8.8642E+08	1.0114E+09	9.1268E+08	8.9600E+08	7.6055E+08	4.5329E+08	8.1487E+08	5.7414E+09	3.8309E+09
27.38	0.0000E+00	0.0000E+00	0.0000E+00	6.0080E+06	2.8487E+07	5.6146E+07	8.9347E+08	7.0622E+09	3.7753E+09
31.62	4.0311E+08	1.1180E+08	1.3161E+07	3.4748E+07	1.2288E+08	5.2998E+08	1.8998E+09	9.4988E+09	3.5780E+09
36.52	3.3502E+09	2.1904E+09	1.4862E+09	1.3804E+09	1.5720E+09	2.2585E+09	3.8119E+09	1.2685E+10	3.2607E+09
42.17	8.9988E+09	6.5841E+09	4.9948E+09	4.6785E+09	4.7031E+09	5.2758E+09	6.4187E+09	1.6019E+10	2.8329E+09
48.7	1.6918E+10	1.3110E+10	1.0582E+10	1.0035E+10	9.4508E+09	9.3523E+09	9.3640E+09	1.8782E+10	2.2986E+09
56.23	2.5199E+10	2.0337E+10	1.7144E+10	1.6437E+10	1.4828E+10	1.3546E+10	1.1887E+10	2.0083E+10	1.7075E+09
64.94	3.1439E+10	2.6243E+10	2.2890E+10	2.2151E+10	1.9351E+10	1.6663E+10	1.3236E+10	1.9396E+10	1.1328E+09
74.99	3.3618E+10	2.8968E+10	2.6039E+10	2.5409E+10	2.1604E+10	1.7696E+10	1.2927E+10	1.6706E+10	6.5009E+08
86.6	3.0966E+10	2.7572E+10	2.5510E+10	2.5092E+10	2.0802E+10	1.6258E+10	1.0997E+10	1.2628E+10	3.0706E+08
100	2.4394E+10	2.2522E+10	2.1470E+10	2.1284E+10	1.7199E+10	1.2809E+10	8.0220E+09	8.1776E+09	1.0879E+08
115.48	1.6094E+10	1.5515E+10	1.5289E+10	1.5282E+10	1.2004E+10	8.4633E+09	4.8661E+09	4.3484E+09	2.3345E+07
133.35	8.5137E+09	8.6800E+09	8.8997E+09	8.9779E+09	6.8165E+09	4.4782E+09	2.3031E+09	1.7374E+09	1.7813E+06
153.99	3.2773E+09	3.6239E+09	3.9121E+09	3.9897E+09	2.8979E+09	1.7107E+09	7.2798E+08	4.0925E+08	9.7444E+05
177.83	6.9304E+08	8.8805E+08	1.0371E+09	1.0736E+09	7.2902E+08	3.4214E+08	7.5162E+07	2.8981E+06	1.3578E+06
205.35	0.0000E+00	0.0000E+00	0.0000E+00	0.0000E+00	0.0000E+00	0.0000E+00	0.0000E+00	2.4486E+05	1.3492E+06
237.14	0.0000E+00	0.0000E+00	0.0000E+00	0.0000E+00	0.0000E+00	0.0000E+00	0.0000E+00	9.3863E+05	1.0510E+06
273.84	0.0000E+00	0.0000E+00	0.0000E+00	0.0000E+00	0.0000E+00	0.0000E+00	0.0000E+00	1.4132E+06	7.4977E+05
316.23	0.0000E+00	0.0000E+00	0.0000E+00	0.0000E+00	0.0000E+00	0.0000E+00	0.0000E+00	1.6333E+06	5.5110E+05
365.17	0.0000E+00	0.0000E+00	0.0000E+00	0.0000E+00	0.0000E+00	0.0000E+00	1.9590E+04	1.8555E+06	4.4395E+05
421.7	0.0000E+00	0.0000E+00	0.0000E+00	6.1301E+03	0.0000E+00	0.0000E+00	1.5338E+05	2.3110E+06	3.6075E+05
486.97	0.0000E+00	0.0000E+00	0.0000E+00	2.4512E+05	0.0000E+00	1.5966E+03	2.6317E+05	2.0515E+06	2.9659E+05
562.34	0.0000E+00	2.5031E+03	6.0383E+03	5.5462E+05	3.8062E+02	4.9957E+03	1.9249E+05	1.0549E+06	2.7118E+05
649.38	9.4175E+02	8.4659E+03	1.3465E+04	4.6795E+05	6.8719E+03	7.3390E+03	4.0603E+03	1.7717E+05	2.5526E+05
749.89	0.0000E+00	0.0000E+00	0.0000E+00	0.0000E+00	0.0000E+00	0.0000E+00	0.0000E+00	2.1508E+05	2.3198E+05
865.96	0.0000E+00	0.0000E+00	0.0000E+00	0.0000E+00	0.0000E+00	0.0000E+00	0.0000E+00	3.7454E+05	1.9348E+05
1000	0.0000E+00	0.0000E+00	0.0000E+00	0.0000E+00	0.0000E+00	0.0000E+00	8.3975E+03	6.3919E+05	1.6277E+05

Table S3: *Averaged measured soot particle size distributions along the centreline of the 5 mol% toluene/heptane flame in dN/dlogD_p (cm^{-3}).*

	HAB (mm)										
D_p (nm)	10	11	12	13	14	15	16	17	18	19	20
4.87	2.6610E+08	5.4392E+08	1.0140E+09	7.4898E+08	2.3610E+08	1.5545E+08	1.8158E+08	2.7060E+08	3.4126E+08	4.7434E+08	3.7734E+08
5.62	4.3008E+08	9.7341E+08	2.6869E+09	2.7331E+09	7.7377E+08	4.0605E+07	4.9856E+06	1.6593E+08	8.0178E+08	1.5939E+09	1.4529E+09
6.49	4.4709E+08	1.0686E+09	4.1247E+09	5.5750E+09	3.1260E+09	1.2395E+09	2.2888E+08	3.8676E+08	1.0361E+09	1.8593E+09	1.7226E+09
7.5	3.5790E+08	8.4657E+08	4.5070E+09	8.3499E+09	8.7811E+09	8.0039E+09	5.3104E+09	3.6118E+09	1.7532E+09	8.3849E+08	3.8250E+08
8.66	2.1194E+08	4.7284E+08	3.8183E+09	1.0016E+10	1.5793E+10	1.8498E+10	1.4633E+10	1.0959E+10	5.2761E+09	1.7123E+09	1.3442E+08
10	1.0094E+08	1.7224E+08	2.6172E+09	9.8043E+09	2.0337E+10	2.7526E+10	2.4978E+10	2.2110E+10	1.4062E+10	9.0106E+09	4.5877E+09
11.55	5.4961E+07	4.9159E+07	1.4939E+09	7.7060E+09	1.9866E+10	3.0707E+10	3.2576E+10	3.4648E+10	2.7720E+10	2.4123E+10	1.7352E+10
13.34	4.4601E+07	3.0929E+07	6.8815E+08	4.6672E+09	1.5203E+10	2.7632E+10	3.5102E+10	4.4251E+10	4.1533E+10	4.2101E+10	3.4840E+10
15.4	4.5093E+07	3.1149E+07	2.0943E+08	1.9608E+09	9.0753E+09	2.0582E+10	3.1916E+10	4.6745E+10	4.9433E+10	5.5372E+10	5.0045E+10
17.78	4.4782E+07	3.3296E+07	1.9489E+07	4.4716E+08	4.1456E+09	1.2648E+10	2.4160E+10	4.0584E+10	4.7751E+10	5.8437E+10	5.7013E+10
20.54	3.9207E+07	3.0728E+07	1.1131E+07	2.9333E+07	1.3483E+09	6.1278E+09	1.4794E+10	2.8876E+10	3.8323E+10	5.1830E+10	5.4853E+10
23.71	3.2524E+07	2.6696E+07	1.1301E+07	8.8883E+05	2.9096E+08	2.1219E+09	7.0362E+09	1.6778E+10	2.6008E+10	3.9848E+10	4.6255E+10
27.38	2.6560E+07	2.2891E+07	1.0392E+07	1.6443E+06	1.9978E+07	4.1465E+08	2.3121E+09	7.5848E+09	1.4721E+10	2.6715E+10	3.4667E+10
31.62	2.2831E+07	2.0513E+07	1.1060E+07	4.8146E+06	4.7903E+04	5.2112E+06	2.5623E+08	2.1659E+09	6.4510E+09	1.5291E+10	2.3009E+10
36.52	2.0265E+07	1.8771E+07	1.2414E+07	9.4949E+06	2.8169E+06	4.1769E+05	0.0000E+00	1.2708E+08	1.8278E+09	7.1323E+09	1.3236E+10
42.17	1.8483E+07	1.7652E+07	1.2950E+07	1.3114E+07	7.9175E+06	1.1889E+06	0.0000E+00	0.0000E+00	1.7781E+08	2.4657E+09	6.3021E+09
48.7	1.7656E+07	1.7101E+07	1.2731E+07	1.4285E+07	1.2659E+07	2.8085E+06	2.5778E+05	0.0000E+00	0.0000E+00	5.1038E+08	2.2901E+09
56.23	1.7392E+07	1.6686E+07	1.2085E+07	1.3507E+07	1.5582E+07	7.3735E+06	1.4690E+06	1.8732E+05	0.0000E+00	2.5540E+07	5.4022E+08
64.94	1.7171E+07	1.5791E+07	1.1328E+07	1.1516E+07	1.5605E+07	1.3372E+07	5.9613E+06	2.3275E+06	2.2734E+04	7.4552E+05	3.0695E+07
74.99	1.6308E+07	1.4173E+07	1.0418E+07	9.4357E+06	1.3335E+07	1.7254E+07	1.2621E+07	7.5256E+06	1.2292E+06	6.2290E+05	0.0000E+00
86.6	1.4501E+07	1.1989E+07	8.9341E+06	7.9808E+06	1.0700E+07	1.6629E+07	1.5988E+07	1.3644E+07	4.4670E+06	3.9804E+06	8.0746E+05
100	1.2113E+07	9.8246E+06	7.0810E+06	6.9348E+06	8.4351E+06	1.2504E+07	1.3530E+07	1.5315E+07	8.0097E+06	8.6415E+06	8.0683E+06
115.48	9.5177E+06	7.9808E+06	5.3977E+06	5.8083E+06	6.9200E+06	8.1044E+06	7.7587E+06	1.0992E+07	8.5309E+06	1.1370E+07	1.1881E+07
133.35	7.3246E+06	6.4415E+06	4.1571E+06	4.5497E+06	5.7699E+06	6.1470E+06	4.0512E+06	4.6619E+06	5.4548E+06	1.0282E+07	1.1040E+07
153.99	5.6836E+06	4.9603E+06	3.2795E+06	3.2766E+06	4.7377E+06	5.2459E+06	3.4931E+06	2.6335E+06	2.0259E+06	6.5015E+06	7.1800E+06
177.83	4.4379E+06	3.6917E+06	2.6542E+06	2.2648E+06	3.7326E+06	4.5811E+06	3.9439E+06	2.8641E+06	1.2548E+06	3.2349E+06	3.0788E+06
205.35	3.5417E+06	2.7315E+06	2.1176E+06	1.6385E+06	2.8609E+06	3.8469E+06	4.3214E+06	4.1445E+06	1.8501E+06	2.2181E+06	1.1002E+06
237.14	2.8421E+06	2.0910E+06	1.7063E+06	1.3519E+06	2.1921E+06	3.0713E+06	4.0740E+06	4.7938E+06	2.9349E+06	2.4334E+06	9.8916E+05
273.84	2.2926E+06	1.6882E+06	1.3970E+06	1.2169E+06	1.7649E+06	2.4304E+06	3.4187E+06	4.5004E+06	3.3848E+06	3.1042E+06	1.5648E+06
316.23	1.8681E+06	1.4479E+06	1.1400E+06	1.0749E+06	1.5495E+06	1.9927E+06	2.6632E+06	3.6332E+06	3.0606E+06	3.3643E+06	2.2955E+06
365.17	1.5414E+06	1.2512E+06	8.9117E+05	8.7855E+05	1.3669E+06	1.6926E+06	1.9973E+06	2.6662E+06	2.3183E+06	2.9961E+06	2.5141E+06
421.7	1.3005E+06	1.0489E+06	6.8434E+05	6.9275E+05	1.1251E+06	1.4100E+06	1.4593E+06	1.8644E+06	1.5563E+06	2.2626E+06	2.1696E+06
486.97	1.1023E+06	8.3485E+05	5.1885E+05	5.5988E+05	8.5862E+05	1.1300E+06	1.0763E+06	1.2872E+06	9.9144E+05	1.5108E+06	1.5437E+06
562.34	9.3473E+05	6.2901E+05	4.1400E+05	4.6716E+05	6.3611E+05	8.7598E+05	8.2135E+05	8.9815E+05	6.4569E+05	9.4627E+05	9.5363E+05
649.38	7.9302E+05	4.8301E+05	3.5049E+05	3.9573E+05	5.0249E+05	6.9485E+05	6.5954E+05	6.8642E+05	4.8995E+05	6.0694E+05	5.6784E+05
749.89	6.9999E+05	4.1180E+05	3.2052E+05	3.4909E+05	4.4880E+05	6.0553E+05	5.8069E+05	6.1256E+05	4.6952E+05	4.8112E+05	4.1584E+05
865.96	6.6605E+05	3.9084E+05	2.9877E+05	3.1871E+05	4.3780E+05	5.8499E+05	5.7337E+05	6.3814E+05	5.1305E+05	5.0937E+05	4.0538E+05
1000	6.9026E+05	4.0580E+05	3.0433E+05	3.0818E+05	4.6387E+05	6.2015E+05	6.5208E+05	7.7813E+05	6.1646E+05	7.0225E+05	5.1370E+05

	HAB (mm)										
D_p (nm)	21	22	23	24	25	26	27	28	29	30	31
4.87	2.8673E+08	1.5456E+08	1.5992E+08	1.1907E+08	1.1213E+08	7.6868E+07	7.8152E+07	6.7329E+07	5.1647E+07	5.8523E+07	6.3389E+07
5.62	1.0670E+09	6.6396E+08	5.7902E+08	3.2722E+08	2.2822E+08	1.5292E+08	1.2729E+08	9.7961E+07	7.0032E+07	8.0076E+07	8.5615E+07
6.49	1.3004E+09	9.0356E+08	7.9794E+08	4.7142E+08	3.0008E+08	2.0841E+08	1.3721E+08	1.0672E+08	7.9714E+07	8.3428E+07	8.5451E+07
7.5	2.3385E+08	1.6631E+08	2.2494E+08	2.4858E+08	1.8422E+08	1.1044E+08	4.8509E+07	5.6949E+07	5.7434E+07	5.6950E+07	5.8269E+07
8.66	1.7472E+06	0.0000E+00	0.0000E+00	2.3570E+06	1.1968E+07	2.9102E+06	0.0000E+00	0.0000E+00	0.0000E+00	9.3786E+05	2.2824E+06
10	2.1753E+09	5.4208E+08	2.9696E+08	8.9645E+07	1.5053E+08	9.1196E+07	0.0000E+00	0.0000E+00	0.0000E+00	0.0000E+00	0.0000E+00
11.55	1.2523E+10	8.6467E+09	6.9476E+09	3.5512E+09	2.2057E+09	1.9837E+09	1.1385E+09	3.8123E+08	3.9093E+07	1.2841E+06	9.2851E+05
13.34	2.8623E+10	2.2919E+10	1.9404E+10	1.1373E+10	7.3080E+09	6.2739E+09	3.7067E+09	2.0630E+09	1.0834E+09	4.7469E+08	3.3052E+08
15.4	4.4581E+10	3.9019E+10	3.4581E+10	2.3156E+10	1.5956E+10	1.2759E+10	6.4180E+09	3.7312E+09	2.3691E+09	1.4157E+09	1.0969E+09
17.78	5.4629E+10	5.1928E+10	4.8378E+10	3.7055E+10	2.7550E+10	2.0800E+10	8.0790E+09	3.9149E+09	2.7719E+09	2.2179E+09	1.8437E+09
20.54	5.6735E+10	5.8632E+10	5.7573E+10	4.9949E+10	4.0014E+10	2.9664E+10	9.0658E+09	2.7121E+09	1.9647E+09	2.2129E+09	1.9373E+09
23.71	5.1927E+10	5.8323E+10	6.0437E+10	5.8690E+10	5.0687E+10	3.8489E+10	1.0688E+10	1.5271E+09	4.8204E+08	1.1750E+09	1.0856E+09
27.38	4.2668E+10	5.2208E+10	5.7251E+10	6.1750E+10	5.7491E+10	4.5983E+10	1.3807E+10	2.1810E+09	2.2811E+06	0.0000E+00	0.0000E+00
31.62	3.1680E+10	4.2567E+10	4.9643E+10	5.9220E+10	5.9346E+10	5.0766E+10	1.8474E+10	5.9921E+09	1.3864E+09	1.1267E+08	3.1752E+06
36.52	2.1043E+10	3.1469E+10	3.9408E+10	5.2087E+10	5.6349E+10	5.2212E+10	2.3979E+10	1.2688E+10	5.9932E+09	2.5008E+09	1.4671E+09
42.17	1.2216E+10	2.0812E+10	2.8450E+10	4.1954E+10	4.9271E+10	5.0039E+10	2.9288E+10	2.1381E+10	1.3803E+10	7.6307E+09	5.3139E+09
48.7	6.0162E+09	1.2134E+10	1.8529E+10	3.0719E+10	3.9347E+10	4.4303E+10	3.3221E+10	3.0746E+10	2.4139E+10	1.5332E+10	1.1822E+10
56.23	2.3812E+09	6.0835E+09	1.0751E+10	2.0240E+10	2.8438E+10	3.5911E+10	3.4398E+10	3.8170E+10	3.4450E+10	2.3962E+10	1.9915E+10
64.94	7.0390E+08	2.5358E+09	5.4608E+09	1.1786E+10	1.8312E+10	2.6320E+10	3.2159E+10	4.1331E+10	4.1700E+10	3.1130E+10	2.7503E+10
74.99	1.3795E+08	8.5143E+08	2.3806E+09	5.9161E+09	1.0283E+10	1.7136E+10	2.6738E+10	3.8977E+10	4.3470E+10	3.4599E+10	3.2317E+10
86.6	7.8963E+06	2.2597E+08	8.7383E+08	2.4644E+09	4.8711E+09	9.6549E+09	1.9401E+10	3.1716E+10	3.9067E+10	3.3171E+10	3.2736E+10
100	1.1061E+07	4.8880E+07	2.5734E+08	7.9921E+08	1.8288E+09	4.5042E+09	1.1947E+10	2.1832E+10	2.9948E+10	2.7311E+10	2.8580E+10
115.48	3.2220E+07	3.4407E+07	7.7911E+07	1.8362E+08	4.7181E+08	1.5942E+09	5.9395E+09	1.2217E+10	1.9083E+10	1.8985E+10	2.1247E+10
133.35	3.3963E+07	3.9412E+07	4.8318E+07	4.3497E+07	5.3630E+07	3.3789E+08	2.1403E+09	5.0985E+09	9.5667E+09	1.0736E+10	1.3070E+10
153.99	2.2105E+07	3.1144E+07	4.3936E+07	4.5298E+07	1.2012E+07	8.3229E+06	4.0257E+08	1.2438E+09	3.3144E+09	4.5456E+09	6.2379E+09
177.83	9.3527E+06	1.5890E+07	3.2069E+07	5.2994E+07	4.3920E+07	2.1532E+06	0.0000E+00	0.0000E+00	4.8735E+08	1.1389E+09	1.9624E+09
205.35	2.5502E+06	4.5860E+06	1.6465E+07	4.0892E+07	5.6125E+07	2.0446E+07	0.0000E+00	0.0000E+00	0.0000E+00	1.4428E+06	1.7426E+08
237.14	1.4281E+06	4.6156E+05	5.5051E+06	2.1521E+07	4.1594E+07	3.4889E+07	1.8187E+05	0.0000E+00	0.0000E+00	0.0000E+00	0.0000E+00
273.84	1.7699E+06	1.0917E+05	1.0985E+06	7.1079E+06	1.9814E+07	2.9692E+07	1.6137E+06	0.0000E+00	0.0000E+00	0.0000E+00	0.0000E+00
316.23	2.4751E+06	3.0899E+05	8.3687E+05	9.6310E+05	5.2977E+06	1.6856E+07	2.7518E+06	0.0000E+00	0.0000E+00	0.0000E+00	0.0000E+00
365.17	2.8676E+06	6.1952E+05	1.3466E+06	2.3172E+05	4.8300E+05	5.8761E+06	4.2817E+06	1.8122E+04	0.0000E+00	0.0000E+00	0.0000E+00
421.7	2.6286E+06	8.1406E+05	1.5338E+06	5.1351E+05	6.4452E+04	8.5149E+05	4.6332E+06	1.0803E+05	0.0000E+00	0.0000E+00	0.0000E+00
486.97	1.9310E+06	8.0667E+05	1.3717E+06	7.6033E+05	1.6701E+05	9.7529E+03	2.5596E+06	3.4958E+05	2.3642E+04	0.0000E+00	0.0000E+00
562.34	1.1608E+06	6.6034E+05	1.0358E+06	8.4588E+05	3.6590E+05	0.0000E+00	3.9770E+04	2.1351E+05	2.8932E+04	6.5429E+03	2.6630E+04
649.38	6.2007E+05	4.8734E+05	7.2904E+05	8.4524E+05	5.8053E+05	2.2973E+04	0.0000E+00	0.0000E+00	0.0000E+00	3.3124E+04	3.7988E+04
749.89	4.0087E+05	3.6401E+05	5.5788E+05	8.0038E+05	7.3246E+05	1.3798E+05	0.0000E+00	0.0000E+00	0.0000E+00	0.0000E+00	0.0000E+00
865.96	4.3645E+05	3.1025E+05	4.9308E+05	7.6984E+05	8.1798E+05	3.0187E+05	4.8509E+03	0.0000E+00	0.0000E+00	0.0000E+00	0.0000E+00
1000	6.8137E+05	3.1659E+05	5.6023E+05	7.8385E+05	8.5680E+05	4.5876E+05	2.2157E+05	1.3221E+04	0.0000E+00	0.0000E+00	0.0000E+00

	HAB (mm)								
D_p (nm)	32	33	34	35	36	37	38	39	40
4.87	5.6949E+07	5.6645E+07	6.0415E+07	5.6248E+07	5.0065E+07	5.2806E+07	5.3703E+07	4.8402E+07	5.7395E+07
5.62	7.6635E+07	6.9446E+07	7.3143E+07	6.5596E+07	5.9853E+07	6.5197E+07	7.0076E+07	6.6969E+07	8.0169E+07
6.49	7.7224E+07	7.0095E+07	6.8160E+07	5.9641E+07	5.7889E+07	6.6503E+07	6.6415E+07	6.9118E+07	7.8697E+07
7.5	5.8522E+07	6.1090E+07	6.2112E+07	5.7722E+07	5.6349E+07	5.8027E+07	4.8503E+07	4.7515E+07	5.1706E+07
8.66	1.5649E+07	3.2221E+07	4.2188E+07	4.1266E+07	4.0234E+07	3.0541E+07	1.4936E+07	8.3217E+06	2.0131E+07
10	6.9030E+05	6.9326E+06	1.7121E+07	2.0014E+07	1.8628E+07	1.0033E+07	2.0885E+06	3.9305E+06	4.6089E+07
11.55	4.3126E+05	5.2469E+05	1.2160E+06	2.6878E+06	3.0482E+06	5.1236E+06	1.8638E+07	7.6636E+07	2.2639E+08
13.34	1.8711E+08	1.1781E+07	3.2949E+06	2.5732E+06	1.0880E+07	5.2763E+07	1.8213E+08	3.2650E+08	5.0405E+08
15.4	7.0100E+08	3.6693E+08	2.8485E+08	2.2572E+08	2.4830E+08	3.4233E+08	5.1127E+08	6.2655E+08	7.3132E+08
17.78	1.2618E+09	1.0789E+09	8.9879E+08	7.3615E+08	7.4739E+08	8.1765E+08	8.2696E+08	7.8889E+08	8.0005E+08
20.54	1.3967E+09	1.6144E+09	1.3892E+09	1.1548E+09	1.1355E+09	1.1125E+09	8.8292E+08	7.2694E+08	7.5984E+08
23.71	8.4315E+08	1.4055E+09	1.2436E+09	1.0453E+09	1.0022E+09	8.8916E+08	5.6361E+08	5.0880E+08	7.5970E+08
27.38	5.8183E+07	6.1082E+08	5.7125E+08	4.8920E+08	4.5024E+08	3.2359E+08	1.4919E+08	3.9523E+08	9.3954E+08
31.62	0.0000E+00	0.0000E+00	0.0000E+00	0.0000E+00	5.4150E+05	2.6877E+06	1.4473E+08	6.9615E+08	1.3713E+09
36.52	7.3016E+08	1.0539E+08	3.1964E+07	3.0700E+06	5.5306E+07	1.9790E+08	7.5585E+08	1.4917E+09	2.0068E+09
42.17	3.0881E+09	1.8731E+09	1.3771E+09	1.0610E+09	1.1748E+09	1.5533E+09	2.1948E+09	2.7697E+09	2.7481E+09
48.7	7.4389E+09	5.6722E+09	4.4569E+09	3.5902E+09	3.7717E+09	4.3246E+09	4.5102E+09	4.4319E+09	3.4666E+09
56.23	1.3227E+10	1.1098E+10	9.0405E+09	7.4468E+09	7.6728E+09	8.2072E+09	7.3316E+09	6.1232E+09	3.9608E+09
64.94	1.9054E+10	1.6916E+10	1.4149E+10	1.1828E+10	1.2045E+10	1.2306E+10	9.9612E+09	7.3878E+09	4.0717E+09
74.99	2.3240E+10	2.1544E+10	1.8427E+10	1.5580E+10	1.5717E+10	1.5488E+10	1.1634E+10	7.8296E+09	3.7320E+09
86.6	2.4412E+10	2.3520E+10	2.0542E+10	1.7533E+10	1.7533E+10	1.6730E+10	1.1789E+10	7.2784E+09	3.0144E+09
100	2.2142E+10	2.2163E+10	1.9764E+10	1.7014E+10	1.6861E+10	1.5588E+10	1.0343E+10	5.8838E+09	2.1075E+09
115.48	1.7198E+10	1.7931E+10	1.6348E+10	1.4187E+10	1.3920E+10	1.2445E+10	7.7608E+09	4.0605E+09	1.2364E+09
133.35	1.1193E+10	1.2232E+10	1.1436E+10	1.0005E+10	9.7018E+09	8.3430E+09	4.8446E+09	2.3069E+09	5.7267E+08
153.99	5.8275E+09	6.7657E+09	6.5230E+09	5.7566E+09	5.4984E+09	4.5004E+09	2.3727E+09	9.9720E+08	1.8179E+08
177.83	2.1891E+09	2.7821E+09	2.7963E+09	2.4933E+09	2.3320E+09	1.7784E+09	7.9298E+08	2.6470E+08	2.3333E+07
205.35	4.3310E+08	6.6308E+08	7.1342E+08	6.4540E+08	5.8327E+08	3.9184E+08	1.0350E+08	5.5536E+06	1.9755E+04
237.14	0.0000E+00	0.0000E+00	0.0000E+00	0.0000E+00	0.0000E+00	0.0000E+00	0.0000E+00	0.0000E+00	1.0228E+05
273.84	0.0000E+00	0.0000E+00	0.0000E+00	0.0000E+00	0.0000E+00	0.0000E+00	0.0000E+00	0.0000E+00	2.6911E+05
316.23	0.0000E+00	0.0000E+00	0.0000E+00	0.0000E+00	0.0000E+00	0.0000E+00	0.0000E+00	0.0000E+00	4.2110E+05
365.17	0.0000E+00	0.0000E+00	0.0000E+00	0.0000E+00	0.0000E+00	0.0000E+00	0.0000E+00	0.0000E+00	6.7084E+05
421.7	0.0000E+00	0.0000E+00	0.0000E+00	0.0000E+00	0.0000E+00	0.0000E+00	0.0000E+00	2.9299E+04	9.0611E+05
486.97	0.0000E+00	0.0000E+00	0.0000E+00	0.0000E+00	0.0000E+00	0.0000E+00	5.5925E+03	1.5624E+05	8.3987E+05
562.34	8.8054E+02	0.0000E+00	0.0000E+00	0.0000E+00	0.0000E+00	0.0000E+00	5.4188E+04	2.7477E+05	4.7655E+05
649.38	1.1478E+04	2.0236E+04	4.5967E+04	2.7660E+04	1.5263E+04	2.1377E+03	7.4999E+04	1.8896E+05	1.0734E+05
749.89	2.3258E+04	6.5763E+04	1.1987E+05	9.4384E+04	5.8838E+04	2.2221E+04	0.0000E+00	0.0000E+00	9.5882E+04
865.96	0.0000E+00	0.0000E+00	0.0000E+00	0.0000E+00	0.0000E+00	0.0000E+00	0.0000E+00	0.0000E+00	1.2483E+05
1000	0.0000E+00	0.0000E+00	0.0000E+00	0.0000E+00	0.0000E+00	0.0000E+00	0.0000E+00	5.7040E+03	2.1438E+05

Table S4: *Averaged measured soot particle size distributions along the centreline of the 10 mol% toluene/heptane flame in dN/dlogD_p (cm^{-3}).*

	HAB (mm)										
D_p (nm)	10	11	12	13	14	15	16	17	18	19	20
4.87	3.5054E+08	7.4079E+08	9.6481E+08	2.9731E+08	1.2010E+08	1.5889E+08	2.1988E+08	3.7303E+08	3.5298E+08	1.5684E+08	1.8641E+08
5.62	5.9723E+08	1.5365E+09	2.8486E+09	1.1166E+09	2.6075E+07	5.1973E+06	2.8140E+08	1.1320E+09	1.2880E+09	1.1116E+09	8.2142E+08
6.49	6.4746E+08	1.9518E+09	4.8066E+09	3.5950E+09	1.1168E+09	9.8515E+07	4.4216E+08	1.3632E+09	1.5301E+09	1.3584E+09	1.0681E+09
7.5	5.2452E+08	1.7959E+09	5.8649E+09	8.2495E+09	7.1928E+09	4.3528E+09	2.4875E+09	1.2886E+09	5.8925E+08	2.6862E+08	9.4789E+07
8.66	3.0677E+08	1.2340E+09	5.7055E+09	1.3341E+10	1.6520E+10	1.2711E+10	7.8965E+09	3.7982E+09	1.2165E+09	2.3850E+08	0.0000E+00
10	1.3275E+08	6.2670E+08	4.5942E+09	1.6014E+10	2.4316E+10	2.2672E+10	1.7334E+10	1.2520E+10	6.8811E+09	3.3737E+09	9.9201E+08
11.55	5.6565E+07	2.3567E+08	3.0581E+09	1.4633E+10	2.6654E+10	3.0835E+10	2.9228E+10	2.7736E+10	2.0095E+10	1.4551E+10	1.0870E+10
13.34	3.4727E+07	6.9886E+07	1.5972E+09	1.0234E+10	2.3374E+10	3.4548E+10	3.9379E+10	4.4174E+10	3.6685E+10	3.0367E+10	2.6991E+10
15.4	3.6843E+07	3.5937E+07	5.6524E+08	5.2389E+09	1.6797E+10	3.2512E+10	4.3230E+10	5.4576E+10	4.9557E+10	4.4374E+10	4.3245E+10
17.78	4.0198E+07	3.5233E+07	8.4839E+07	1.7772E+09	9.8487E+09	2.5335E+10	3.8672E+10	5.4238E+10	5.3255E+10	5.0999E+10	5.3565E+10
20.54	3.5653E+07	3.4147E+07	9.6713E+06	2.7516E+08	4.4667E+09	1.5950E+10	2.8335E+10	4.4781E+10	4.7955E+10	4.9336E+10	5.5806E+10
23.71	2.9374E+07	3.0594E+07	1.2183E+07	1.3200E+07	1.3736E+09	7.8651E+09	1.7092E+10	3.1447E+10	3.7452E+10	4.1784E+10	5.1014E+10
27.38	2.3983E+07	2.6410E+07	1.4623E+07	0.0000E+00	2.0807E+08	2.7607E+09	8.2119E+09	1.8673E+10	2.5611E+10	3.1473E+10	4.1713E+10
31.62	2.1132E+07	2.3974E+07	2.0195E+07	5.5400E+05	0.0000E+00	4.1518E+08	2.7127E+09	8.8938E+09	1.5117E+10	2.1068E+10	3.0685E+10
36.52	1.9108E+07	2.2229E+07	2.4772E+07	5.7812E+06	2.1906E+05	0.0000E+00	3.9920E+08	3.0376E+09	7.4559E+09	1.2334E+10	2.0060E+10
42.17	1.7787E+07	2.0977E+07	2.5743E+07	1.3139E+07	1.3717E+06	0.0000E+00	4.8531E+06	5.5471E+08	2.9040E+09	6.1099E+09	1.1321E+10
48.7	1.6964E+07	2.0364E+07	2.4142E+07	1.8482E+07	3.9594E+06	2.8749E+03	0.0000E+00	1.4885E+07	7.9167E+08	2.4614E+09	5.2856E+09
56.23	1.6159E+07	1.9880E+07	2.1430E+07	1.9851E+07	8.6922E+06	3.0449E+05	0.0000E+00	0.0000E+00	1.0423E+08	7.1272E+08	1.8674E+09
64.94	1.5150E+07	1.9154E+07	1.8624E+07	1.7536E+07	1.3295E+07	2.3130E+06	3.0443E+04	1.0651E+04	2.5022E+05	1.0540E+08	4.2235E+08
74.99	1.3717E+07	1.7746E+07	1.6120E+07	1.3563E+07	1.4734E+07	6.2042E+06	6.1065E+05	4.5847E+05	1.6711E+05	8.7363E+05	4.0793E+07
86.6	1.2019E+07	1.5529E+07	1.3915E+07	1.0584E+07	1.2805E+07	8.3156E+06	2.3871E+06	1.6934E+06	1.4235E+06	5.3106E+05	5.7179E+05
100	1.0269E+07	1.2882E+07	1.1888E+07	9.2769E+06	9.2796E+06	6.8966E+06	4.0784E+06	2.8713E+06	3.3899E+06	2.3218E+06	1.6567E+06
115.48	8.4443E+06	1.0168E+07	9.7403E+06	8.4867E+06	6.3121E+06	3.4128E+06	3.5377E+06	2.9376E+06	4.2501E+06	6.0977E+06	1.2442E+07
133.35	6.7383E+06	7.9006E+06	7.7398E+06	7.3571E+06	4.8987E+06	1.6487E+06	1.5592E+06	1.8201E+06	3.3650E+06	5.6168E+06	1.2593E+07
153.99	5.1272E+06	6.1343E+06	5.9860E+06	5.7971E+06	4.1981E+06	1.5932E+06	6.7964E+05	9.1820E+05	1.9515E+06	3.1732E+06	7.6787E+06
177.83	3.8563E+06	4.7735E+06	4.5158E+06	4.2334E+06	3.6495E+06	2.2752E+06	1.0071E+06	7.6337E+05	1.0480E+06	1.3090E+06	2.8441E+06
205.35	3.0326E+06	3.6819E+06	3.4085E+06	3.0379E+06	3.0647E+06	2.7943E+06	1.8837E+06	1.4296E+06	1.0977E+06	5.7207E+05	4.9366E+05
237.14	2.4397E+06	2.8185E+06	2.7002E+06	2.2414E+06	2.3979E+06	2.7075E+06	2.2910E+06	1.9769E+06	1.5503E+06	8.4470E+05	2.5881E+05
273.84	2.0208E+06	2.2294E+06	2.2290E+06	1.7470E+06	1.8018E+06	2.1824E+06	2.0682E+06	2.0411E+06	1.8949E+06	1.2900E+06	4.5797E+05
316.23	1.7379E+06	1.8907E+06	1.9275E+06	1.4825E+06	1.4008E+06	1.5663E+06	1.5431E+06	1.6945E+06	1.8863E+06	1.5290E+06	7.7538E+05
365.17	1.4938E+06	1.6776E+06	1.6608E+06	1.3123E+06	1.1206E+06	1.0787E+06	1.0353E+06	1.2486E+06	1.5554E+06	1.4369E+06	9.5144E+05
421.7	1.2503E+06	1.4510E+06	1.3726E+06	1.1282E+06	9.2349E+05	7.7698E+05	7.0093E+05	8.8964E+05	1.1197E+06	1.1228E+06	8.6756E+05
486.97	1.0016E+06	1.1770E+06	1.0707E+06	9.1501E+05	7.6668E+05	5.9049E+05	5.2543E+05	6.3403E+05	7.4414E+05	7.7129E+05	6.5621E+05
562.34	7.8389E+05	9.2930E+05	7.9347E+05	7.1042E+05	6.1703E+05	4.8467E+05	4.4423E+05	4.6355E+05	5.0024E+05	5.0955E+05	4.6263E+05
649.38	6.3316E+05	7.7443E+05	6.0858E+05	5.6144E+05	4.8725E+05	4.1476E+05	4.2466E+05	3.8631E+05	3.8907E+05	3.5986E+05	3.4896E+05
749.89	5.6102E+05	7.0715E+05	5.1377E+05	4.8175E+05	4.0947E+05	3.8239E+05	4.1748E+05	3.6842E+05	3.7577E+05	3.0499E+05	2.9442E+05
865.96	5.3537E+05	6.9608E+05	4.9433E+05	4.4363E+05	3.9068E+05	3.7765E+05	4.0263E+05	3.6900E+05	4.1055E+05	3.1322E+05	2.7088E+05
1000	5.4094E+05	7.1317E+05	5.3761E+05	4.6097E+05	4.2237E+05	3.9777E+05	4.0116E+05	3.8869E+05	4.6441E+05	3.6184E+05	2.6365E+05

	HAB (mm)										
D_p (nm)	21	22	23	24	25	26	27	28	29	30	31
4.87	1.3133E+08	9.9694E+07	7.5984E+07	5.0252E+07	5.5741E+07	6.0435E+07	4.2542E+07	4.5075E+07	4.6246E+07	5.7588E+07	6.2893E+07
5.62	5.2779E+08	3.2451E+08	1.6726E+08	8.8019E+07	7.0259E+07	8.8786E+07	7.5217E+07	5.7989E+07	6.0008E+07	7.4346E+07	6.8968E+07
6.49	7.2521E+08	4.8123E+08	2.5025E+08	1.2791E+08	8.7740E+07	1.1280E+08	9.8208E+07	6.2557E+07	6.8038E+07	8.2186E+07	6.7275E+07
7.5	1.0503E+08	1.5439E+08	1.6352E+08	1.2497E+08	8.9460E+07	7.4327E+07	6.0491E+07	4.5627E+07	5.2178E+07	6.7887E+07	6.4432E+07
8.66	0.0000E+00	1.1257E+07	6.0991E+07	1.2492E+08	7.1726E+07	0.0000E+00	0.0000E+00	2.5470E+06	5.4137E+06	1.9714E+07	3.6313E+07
10	2.4875E+08	5.1564E+07	1.6239E+08	1.8209E+08	1.3542E+08	1.3927E+06	0.0000E+00	0.0000E+00	1.1446E+06	6.4940E+05	1.2047E+07
11.55	7.2063E+09	4.7049E+09	2.4832E+09	1.0613E+09	7.8886E+08	6.6592E+08	4.6937E+08	6.4470E+06	1.1590E+06	4.5902E+05	1.1079E+06
13.34	2.0104E+10	1.5388E+10	8.7370E+09	3.8523E+09	2.9196E+09	2.5465E+09	1.8820E+09	4.7774E+08	2.4982E+08	1.8749E+08	7.2501E+07
15.4	3.4995E+10	3.0194E+10	1.9173E+10	9.0243E+09	6.8191E+09	5.3624E+09	3.7267E+09	1.3628E+09	8.6461E+08	8.1336E+08	5.0529E+08
17.78	4.7100E+10	4.5384E+10	3.2368E+10	1.6384E+10	1.2504E+10	8.6699E+09	5.2672E+09	2.0380E+09	1.5365E+09	1.6265E+09	1.3200E+09
20.54	5.3493E+10	5.7034E+10	4.5145E+10	2.4994E+10	1.9888E+10	1.2413E+10	6.3596E+09	1.9346E+09	1.7063E+09	1.9619E+09	1.8914E+09
23.71	5.3359E+10	6.2317E+10	5.4060E+10	3.3483E+10	2.8567E+10	1.6726E+10	7.4049E+09	9.6198E+08	1.0491E+09	1.3459E+09	1.5803E+09
27.38	4.7795E+10	6.0808E+10	5.7381E+10	4.0309E+10	3.7208E+10	2.1383E+10	8.9805E+09	1.5586E+07	1.2599E+08	2.7577E+08	6.3173E+08
31.62	3.8926E+10	5.3925E+10	5.5136E+10	4.4163E+10	4.4033E+10	2.5812E+10	1.1574E+10	4.1538E+08	9.2551E+06	3.6160E+05	0.0000E+00
36.52	2.8689E+10	4.3487E+10	4.8281E+10	4.4606E+10	4.7974E+10	2.9409E+10	1.4848E+10	2.5976E+09	1.1663E+09	6.6837E+08	2.5037E+08
42.17	1.8861E+10	3.1654E+10	3.8453E+10	4.1639E+10	4.8268E+10	3.1580E+10	1.8936E+10	6.9897E+09	4.1257E+09	3.6578E+09	2.3685E+09
48.7	1.0883E+10	2.0588E+10	2.7624E+10	3.5631E+10	4.4516E+10	3.1807E+10	2.3343E+10	1.4031E+10	9.6502E+09	9.5191E+09	7.0208E+09
56.23	5.3568E+09	1.1753E+10	1.7681E+10	2.7719E+10	3.7355E+10	2.9796E+10	2.6897E+10	2.2302E+10	1.6916E+10	1.7545E+10	1.3848E+10
64.94	2.1607E+09	5.7048E+09	9.8538E+09	1.9343E+10	2.8216E+10	2.5733E+10	2.8371E+10	2.9495E+10	2.4079E+10	2.5800E+10	2.1364E+10
74.99	6.8520E+08	2.2296E+09	4.6174E+09	1.1881E+10	1.8875E+10	2.0235E+10	2.6967E+10	3.3303E+10	2.8990E+10	3.1918E+10	2.7537E+10
86.6	1.7049E+08	6.3088E+08	1.7106E+09	6.2369E+09	1.0906E+10	1.4258E+10	2.2745E+10	3.2356E+10	2.9981E+10	3.3883E+10	3.0411E+10
100	2.6132E+07	1.0560E+08	4.3897E+08	2.6537E+09	5.2158E+09	8.8036E+09	1.6694E+10	2.6931E+10	2.6663E+10	3.0976E+10	2.8979E+10
115.48	2.0688E+07	2.2617E+07	5.6141E+07	8.1936E+08	1.8944E+09	4.5999E+09	1.0344E+10	1.8882E+10	2.0165E+10	2.4186E+10	2.3710E+10
133.35	2.9169E+07	4.5834E+07	2.0651E+07	1.3490E+08	4.1246E+08	1.9100E+09	5.1219E+09	1.0749E+10	1.2617E+10	1.5767E+10	1.6364E+10
153.99	2.4889E+07	5.2959E+07	4.8567E+07	1.3301E+07	5.6616E+06	5.5672E+08	1.8002E+09	4.5802E+09	6.1402E+09	8.1720E+09	9.1665E+09
177.83	1.3326E+07	3.5112E+07	5.1712E+07	1.7073E+07	1.6249E+06	9.0055E+07	3.1456E+08	1.1702E+09	1.9960E+09	3.0154E+09	3.8259E+09
205.35	4.1698E+06	1.3650E+07	3.1646E+07	3.1449E+07	1.9872E+07	1.0629E+07	4.1991E+05	3.5167E+07	2.1535E+08	5.5601E+08	9.3033E+08
237.14	6.0168E+05	2.5517E+06	1.0987E+07	3.1493E+07	3.4884E+07	1.3596E+07	4.7576E+06	0.0000E+00	0.0000E+00	0.0000E+00	0.0000E+00
273.84	1.6408E+05	1.4083E+05	1.3492E+06	2.0969E+07	2.9698E+07	1.4482E+07	6.3374E+06	0.0000E+00	0.0000E+00	0.0000E+00	0.0000E+00
316.23	3.9964E+05	1.4872E+05	2.8510E+04	9.4533E+06	1.6866E+07	1.1016E+07	5.4831E+06	0.0000E+00	0.0000E+00	0.0000E+00	0.0000E+00
365.17	6.8955E+05	4.4208E+05	8.3476E+04	2.0576E+06	5.9061E+06	6.8522E+06	3.2780E+06	0.0000E+00	0.0000E+00	0.0000E+00	0.0000E+00
421.7	8.3731E+05	6.9570E+05	2.0203E+05	7.1521E+04	1.1128E+06	3.4212E+06	1.7287E+06	0.0000E+00	0.0000E+00	0.0000E+00	0.0000E+00
486.97	7.7577E+05	7.7569E+05	3.1363E+05	1.0347E+05	0.0000E+00	1.0643E+06	9.1837E+05	0.0000E+00	0.0000E+00	0.0000E+00	0.0000E+00
562.34	5.9812E+05	7.0160E+05	3.9805E+05	1.2780E+05	0.0000E+00	1.3001E+05	5.1844E+05	0.0000E+00	4.4003E+03	2.2047E+03	9.3749E+02
649.38	4.2548E+05	5.8513E+05	4.6399E+05	1.8103E+05	3.0564E+04	7.2078E+04	0.0000E+00	0.0000E+00	1.8179E+04	9.2317E+03	3.4947E+03
749.89	3.1587E+05	4.9514E+05	4.9747E+05	2.8982E+05	1.2518E+05	1.6328E+05	6.0814E+03	0.0000E+00	0.0000E+00	0.0000E+00	5.1217E+03
865.96	2.7144E+05	4.4068E+05	4.8439E+05	4.1074E+05	2.8700E+05	2.5077E+05	6.9869E+04	0.0000E+00	0.0000E+00	0.0000E+00	0.0000E+00
1000	2.9436E+05	4.3541E+05	4.3983E+05	5.0150E+05	4.2435E+05	3.6012E+05	2.0093E+05	0.0000E+00	0.0000E+00	0.0000E+00	0.0000E+00

	HAB (mm)								
D_p (nm)	32	33	34	35	36	37	38	39	40
4.87	3.4800E+07	4.3998E+07	3.9811E+07	4.1724E+07	3.5658E+07	4.6150E+07	4.1966E+07	3.9801E+07	4.8489E+07
5.62	3.3757E+07	4.4332E+07	4.0523E+07	4.4712E+07	3.7395E+07	4.9560E+07	4.3380E+07	4.4679E+07	5.8404E+07
6.49	3.4307E+07	3.8971E+07	3.9692E+07	4.2553E+07	3.8146E+07	4.7005E+07	4.1350E+07	4.7830E+07	5.5778E+07
7.5	4.3233E+07	4.7383E+07	5.0027E+07	5.1504E+07	4.6543E+07	5.4652E+07	4.8050E+07	4.9242E+07	5.0868E+07
8.66	3.0522E+07	3.6163E+07	3.9403E+07	4.4165E+07	3.6140E+07	4.4026E+07	4.0013E+07	3.5964E+07	3.2602E+07
10	1.5093E+07	2.3046E+07	2.5267E+07	3.3129E+07	2.5563E+07	3.1470E+07	2.9028E+07	2.4628E+07	2.1260E+07
11.55	1.6403E+06	1.9990E+06	2.8680E+06	9.0176E+06	5.6362E+06	7.7117E+06	8.0653E+06	1.1142E+07	2.2528E+07
13.34	6.3277E+06	5.7645E+05	1.7856E+04	7.6759E+04	0.0000E+00	6.3081E+05	2.3667E+06	2.0964E+07	8.4704E+07
15.4	2.2185E+08	1.1398E+08	6.8910E+07	4.8805E+07	2.6274E+07	4.5602E+07	7.7978E+07	1.6039E+08	2.7691E+08
17.78	8.1678E+08	6.3638E+08	5.0907E+08	4.2259E+08	3.7354E+08	4.1240E+08	4.0785E+08	4.8254E+08	5.5584E+08
20.54	1.3190E+09	1.1200E+09	9.4082E+08	8.1558E+08	7.6108E+08	8.0853E+08	7.3427E+08	7.4474E+08	7.2263E+08
23.71	1.1991E+09	1.0664E+09	9.2912E+08	8.4097E+08	8.1547E+08	8.5097E+08	7.3404E+08	6.7853E+08	6.0826E+08
27.38	5.6099E+08	5.3481E+08	5.0200E+08	4.9435E+08	5.1094E+08	5.2174E+08	4.1784E+08	3.4485E+08	3.3041E+08
31.62	0.0000E+00	0.0000E+00	3.4157E+07	8.0688E+07	1.1358E+08	1.0958E+08	6.8549E+07	6.2819E+07	2.0311E+08
36.52	6.5091E+07	0.0000E+00	0.0000E+00	0.0000E+00	0.0000E+00	4.7566E+05	1.9078E+07	1.2427E+08	4.5079E+08
42.17	1.1574E+09	6.2755E+08	4.0187E+08	3.3766E+08	2.5936E+08	3.2433E+08	4.1257E+08	7.4711E+08	1.2376E+09
48.7	4.0383E+09	2.8317E+09	2.1288E+09	1.8158E+09	1.6182E+09	1.7805E+09	1.7728E+09	2.2114E+09	2.6866E+09
56.23	8.7188E+09	6.7939E+09	5.3736E+09	4.6322E+09	4.2827E+09	4.5729E+09	4.2245E+09	4.5091E+09	4.6729E+09
64.94	1.4347E+10	1.1926E+10	9.7067E+09	8.4288E+09	7.9265E+09	8.3460E+09	7.4226E+09	7.2447E+09	6.7977E+09
74.99	1.9510E+10	1.7025E+10	1.4156E+10	1.2365E+10	1.1752E+10	1.2264E+10	1.0642E+10	9.7618E+09	8.5207E+09
86.6	2.2636E+10	2.0596E+10	1.7447E+10	1.5321E+10	1.4676E+10	1.5211E+10	1.2956E+10	1.1317E+10	9.3188E+09
100	2.2657E+10	2.1443E+10	1.8495E+10	1.6322E+10	1.5740E+10	1.6215E+10	1.3597E+10	1.1383E+10	8.9105E+09
115.48	1.9535E+10	1.9242E+10	1.6908E+10	1.4997E+10	1.4552E+10	1.4902E+10	1.2318E+10	9.9094E+09	7.4014E+09
133.35	1.4319E+10	1.4740E+10	1.3222E+10	1.1791E+10	1.1512E+10	1.1713E+10	9.5434E+09	7.3714E+09	5.2548E+09
153.99	8.6595E+09	9.4155E+09	8.6635E+09	7.7742E+09	7.6415E+09	7.7139E+09	6.1812E+09	4.5589E+09	3.0881E+09
177.83	4.0523E+09	4.7795E+09	4.5586E+09	4.1240E+09	4.0872E+09	4.0791E+09	3.1949E+09	2.2162E+09	1.4079E+09
205.35	1.2460E+09	1.7236E+09	1.7480E+09	1.6006E+09	1.6055E+09	1.5704E+09	1.1825E+09	7.4063E+08	4.2529E+08
237.14	1.1643E+08	3.1083E+08	3.6834E+08	3.4533E+08	3.5457E+08	3.2931E+08	2.2273E+08	1.0472E+08	4.7552E+07
273.84	0.0000E+00	0.0000E+00	0.0000E+00	0.0000E+00	0.0000E+00	0.0000E+00	0.0000E+00	0.0000E+00	0.0000E+00
316.23	0.0000E+00	0.0000E+00	0.0000E+00	0.0000E+00	0.0000E+00	0.0000E+00	0.0000E+00	0.0000E+00	0.0000E+00
365.17	0.0000E+00	0.0000E+00	0.0000E+00	0.0000E+00	0.0000E+00	0.0000E+00	0.0000E+00	0.0000E+00	0.0000E+00
421.7	0.0000E+00	0.0000E+00	0.0000E+00	0.0000E+00	0.0000E+00	0.0000E+00	0.0000E+00	0.0000E+00	0.0000E+00
486.97	0.0000E+00	0.0000E+00	0.0000E+00	0.0000E+00	0.0000E+00	0.0000E+00	0.0000E+00	0.0000E+00	1.3017E+03
562.34	0.0000E+00	0.0000E+00	0.0000E+00	0.0000E+00	0.0000E+00	0.0000E+00	0.0000E+00	2.9631E+03	8.6206E+03
649.38	8.9065E+03	0.0000E+00	0.0000E+00	0.0000E+00	0.0000E+00	5.7165E+03	1.0168E+03	1.6885E+04	7.1090E+04
749.89	4.1789E+04	2.9729E+04	9.3398E+04	1.6018E+05	1.0539E+05	1.4478E+05	1.0854E+05	1.2037E+05	1.8310E+05
865.96	4.5519E+03	1.3421E+04	1.4130E+05	2.0247E+05	1.4655E+05	1.7427E+05	1.3556E+05	1.0842E+05	1.0708E+05
1000	0.0000E+00	0.0000E+00	0.0000E+00	0.0000E+00	0.0000E+00	0.0000E+00	0.0000E+00	0.0000E+00	0.0000E+00

Table S5: *Averaged measured soot particle size distributions along the centreline of the 15 mol% toluene/heptane flame in dN/dlogD_p (cm^{-3}).*

	HAB (mm)										
D_p (nm)	8	9	10	11	12	13	14	15	16	17	18
4.87	8.2456E+07	4.4206E+08	8.7275E+08	6.5531E+08	2.3429E+08	2.1556E+08	3.1163E+08	3.8764E+08	3.5639E+08	2.6052E+08	2.2076E+08
5.62	9.7223E+07	8.7204E+08	2.2027E+09	2.0061E+09	5.2932E+08	1.5250E+08	7.1802E+08	1.2977E+09	1.4443E+09	1.0771E+09	9.1938E+08
6.49	8.3396E+07	1.0641E+09	3.4914E+09	4.3090E+09	2.3594E+09	5.0034E+08	9.6318E+08	1.5626E+09	1.7419E+09	1.3229E+09	1.1768E+09
7.5	7.2561E+07	9.3145E+08	4.2611E+09	8.9153E+09	8.3299E+09	5.1231E+09	2.2978E+09	9.4335E+08	3.3567E+08	1.7087E+08	1.1827E+08
8.66	4.6974E+07	5.7856E+08	4.3033E+09	1.4456E+10	1.6842E+10	1.3992E+10	6.8655E+09	2.5645E+09	2.0840E+08	6.9810E+06	2.1471E+07
10	3.7593E+07	2.5350E+08	3.6717E+09	1.8215E+10	2.4050E+10	2.4812E+10	1.6630E+10	9.9490E+09	4.5543E+09	2.6737E+09	1.4868E+09
11.55	3.8594E+07	1.0149E+08	2.6022E+09	1.8267E+10	2.6770E+10	3.4211E+10	3.0830E+10	2.5348E+10	1.8384E+10	1.4004E+10	1.2372E+10
13.34	3.6098E+07	6.5413E+07	1.4376E+09	1.4990E+10	2.4625E+10	3.9169E+10	4.4508E+10	4.3734E+10	3.7295E+10	3.1366E+10	3.0366E+10
15.4	3.6822E+07	5.9563E+07	5.3572E+08	1.0151E+10	1.9177E+10	3.7860E+10	5.1558E+10	5.7066E+10	5.3405E+10	4.7887E+10	4.8771E+10
17.78	3.7144E+07	5.7291E+07	1.0181E+08	5.6446E+09	1.2665E+10	3.0544E+10	4.8535E+10	5.9470E+10	6.0175E+10	5.7058E+10	6.0738E+10
20.54	3.3259E+07	5.1334E+07	4.5234E+07	2.4693E+09	6.9338E+09	2.0257E+10	3.7816E+10	5.1748E+10	5.6928E+10	5.7183E+10	6.3708E+10
23.71	2.8073E+07	4.4530E+07	4.5719E+07	7.2944E+08	3.0453E+09	1.0893E+10	2.4813E+10	3.8800E+10	4.6992E+10	5.0245E+10	5.8711E+10
27.38	2.2758E+07	3.7408E+07	4.0316E+07	6.6865E+07	9.4946E+08	4.5149E+09	1.3556E+10	2.5209E+10	3.4305E+10	3.9392E+10	4.8489E+10
31.62	1.9090E+07	3.1328E+07	3.3002E+07	5.0144E+06	1.0590E+08	1.1862E+09	5.7634E+09	1.3862E+10	2.2010E+10	2.7611E+10	3.6137E+10
36.52	1.6041E+07	2.6134E+07	2.6603E+07	1.1844E+07	5.2344E+05	1.6031E+08	1.7129E+09	6.1891E+09	1.2122E+10	1.7053E+10	2.4061E+10
42.17	1.3910E+07	2.2387E+07	2.2826E+07	1.7059E+07	2.5588E+06	4.4901E+06	3.8061E+08	2.1265E+09	5.4718E+09	8.9848E+09	1.3969E+10
48.7	1.2757E+07	2.0390E+07	2.2187E+07	1.8093E+07	5.4432E+06	1.6598E+04	1.7716E+07	5.8146E+08	1.8921E+09	3.8509E+09	6.8376E+09
56.23	1.1925E+07	1.9408E+07	2.2955E+07	1.5752E+07	8.8100E+06	2.2782E+05	0.0000E+00	7.8935E+07	4.9459E+08	1.2372E+09	2.6473E+09
64.94	1.1256E+07	1.8809E+07	2.3042E+07	1.2298E+07	1.0957E+07	1.7803E+06	0.0000E+00	0.0000E+00	8.2460E+07	3.0487E+08	7.2895E+08
74.99	1.0334E+07	1.7819E+07	2.1211E+07	9.7712E+06	1.0822E+07	5.7643E+06	1.9641E+05	0.0000E+00	0.0000E+00	4.7674E+07	1.4552E+08
86.6	9.2523E+06	1.6199E+07	1.7694E+07	8.6538E+06	9.3505E+06	8.7542E+06	1.8719E+06	3.5543E+05	6.1624E+03	7.9356E+05	1.5726E+07
100	7.9866E+06	1.3989E+07	1.4030E+07	8.1526E+06	7.3605E+06	7.8376E+06	3.9014E+06	2.1189E+06	1.4006E+06	1.6163E+06	9.7822E+05
115.48	6.7246E+06	1.1445E+07	1.1226E+07	7.3909E+06	5.6493E+06	4.0445E+06	3.7595E+06	3.9660E+06	3.3327E+06	4.0024E+06	8.5725E+06
133.35	5.5399E+06	9.6509E+06	9.0013E+06	6.3330E+06	4.8387E+06	1.7156E+06	1.5235E+06	4.7899E+06	3.9168E+06	4.1959E+06	1.0492E+07
153.99	4.4183E+06	8.1336E+06	6.8133E+06	5.0517E+06	4.1423E+06	1.7903E+06	2.5187E+05	4.0443E+06	2.9491E+06	2.7381E+06	6.5357E+06
177.83	3.3749E+06	6.5224E+06	4.9643E+06	3.7292E+06	3.3383E+06	2.6515E+06	6.6007E+05	3.3985E+06	1.2012E+06	1.2423E+06	2.4253E+06
205.35	2.4564E+06	4.8841E+06	3.6231E+06	2.6498E+06	2.5293E+06	3.1950E+06	1.7798E+06	2.9091E+06	4.6211E+05	3.1702E+05	4.6378E+05
237.14	1.7947E+06	3.5106E+06	2.7900E+06	1.9549E+06	1.8837E+06	2.9599E+06	2.4991E+06	2.4385E+06	6.0745E+05	2.6376E+05	1.7069E+05
273.84	1.3769E+06	2.5855E+06	2.3416E+06	1.5693E+06	1.4526E+06	2.2589E+06	2.4105E+06	2.0343E+06	1.0972E+06	5.4424E+05	2.5995E+05
316.23	1.1474E+06	2.0588E+06	2.0620E+06	1.3398E+06	1.1711E+06	1.5362E+06	1.8506E+06	1.6927E+06	1.4029E+06	8.3498E+05	5.6613E+05
365.17	9.6141E+05	1.7171E+06	1.7760E+06	1.1272E+06	9.6283E+05	1.0233E+06	1.2252E+06	1.3500E+06	1.3301E+06	8.9683E+05	7.6408E+05
421.7	7.5904E+05	1.3583E+06	1.4195E+06	8.9513E+05	7.8768E+05	7.3102E+05	7.5247E+05	9.5262E+05	1.0230E+06	7.5688E+05	7.3901E+05
486.97	5.7231E+05	1.0178E+06	1.0258E+06	6.7897E+05	6.4336E+05	5.7916E+05	4.8412E+05	6.2181E+05	7.0272E+05	5.4810E+05	5.7767E+05
562.34	4.4616E+05	7.3550E+05	6.9540E+05	5.2367E+05	5.3220E+05	5.0074E+05	3.4408E+05	4.0802E+05	4.6981E+05	3.7229E+05	4.0909E+05
649.38	3.8303E+05	5.5797E+05	4.8416E+05	4.3717E+05	4.6649E+05	4.4620E+05	2.9414E+05	3.0404E+05	3.2980E+05	2.6339E+05	2.8149E+05
749.89	4.7031E+05	4.8155E+05	4.1165E+05	4.1429E+05	4.4319E+05	4.2202E+05	3.1853E+05	2.8367E+05	2.6473E+05	2.1841E+05	2.0743E+05
865.96	5.8054E+05	4.9659E+05	4.3972E+05	4.2304E+05	4.4020E+05	4.2565E+05	3.5134E+05	3.0375E+05	2.5787E+05	2.1649E+05	1.8834E+05
1000	6.4573E+05	5.9256E+05	5.6259E+05	4.4973E+05	4.4451E+05	4.5134E+05	3.9083E+05	3.6149E+05	2.9020E+05	2.4168E+05	2.1607E+05

	HAB (mm)										
D_p (nm)	19	20	21	22	23	24	25	26	27	28	29
4.87	1.8470E+08	1.5697E+08	1.0752E+08	6.1451E+07	4.6016E+07	4.9652E+07	3.9253E+07	2.6039E+07	2.9095E+07	2.4942E+07	2.2282E+07
5.62	7.3670E+08	5.6670E+08	3.1441E+08	1.6509E+08	8.0677E+07	6.4549E+07	5.1555E+07	3.9869E+07	4.9756E+07	2.7666E+07	2.7109E+07
6.49	9.7527E+08	7.4329E+08	4.3962E+08	2.6684E+08	1.2555E+08	7.3990E+07	5.7244E+07	5.1884E+07	6.0866E+07	3.2579E+07	3.2853E+07
7.5	1.1267E+08	1.2114E+08	1.7080E+08	1.5460E+08	1.1659E+08	8.4604E+07	4.8886E+07	2.8189E+07	3.2171E+07	2.5873E+07	2.7200E+07
8.66	0.0000E+00	0.0000E+00	1.0151E+07	0.0000E+00	7.5149E+07	9.6043E+07	2.5908E+07	1.2968E+05	5.6804E+05	0.0000E+00	4.8999E+06
10	6.6538E+08	5.0761E+08	3.3447E+07	2.1121E+05	8.7817E+07	1.6479E+08	8.4208E+07	1.1840E+07	8.1615E+06	0.0000E+00	0.0000E+00
11.55	9.8721E+09	7.5214E+09	3.8886E+09	2.4012E+09	1.1403E+09	7.0472E+08	6.4721E+08	5.3018E+08	4.4830E+08	2.0409E+07	0.0000E+00
13.34	2.6261E+10	2.1071E+10	1.2845E+10	8.6928E+09	4.3950E+09	2.5424E+09	2.6446E+09	2.0276E+09	1.7800E+09	7.3880E+08	1.8442E+08
15.4	4.4326E+10	3.7360E+10	2.5856E+10	1.8815E+10	1.0650E+10	6.5277E+09	6.4424E+09	4.2260E+09	3.2606E+09	1.8709E+09	8.1331E+08
17.78	5.7847E+10	5.1359E+10	4.0249E+10	3.1193E+10	1.9754E+10	1.3154E+10	1.1966E+10	6.3206E+09	4.0575E+09	2.5806E+09	1.4955E+09
20.54	6.3662E+10	5.9588E+10	5.2593E+10	4.2894E+10	3.0096E+10	2.2137E+10	1.9340E+10	8.4700E+09	4.0886E+09	2.4054E+09	1.6630E+09
23.71	6.1577E+10	6.0675E+10	5.9934E+10	5.0902E+10	3.9385E+10	3.2419E+10	2.8505E+10	1.1438E+10	4.0560E+09	1.4100E+09	9.8720E+08
27.38	5.3483E+10	5.5475E+10	6.1202E+10	5.3746E+10	4.5700E+10	4.2066E+10	3.8254E+10	1.5633E+10	5.2845E+09	7.0712E+08	0.0000E+00
31.62	4.2160E+10	4.6163E+10	5.6989E+10	5.1503E+10	4.7925E+10	4.8950E+10	4.6679E+10	2.0875E+10	8.2996E+09	1.8378E+09	0.0000E+00
36.52	2.9968E+10	3.4850E+10	4.8606E+10	4.5085E+10	4.6014E+10	5.2031E+10	5.2462E+10	2.6477E+10	1.3767E+10	5.2039E+09	9.3073E+08
42.17	1.8878E+10	2.3583E+10	3.7852E+10	3.5984E+10	4.0527E+10	5.0761E+10	5.4512E+10	3.1538E+10	2.1286E+10	1.1149E+10	4.3198E+09
48.7	1.0320E+10	1.4111E+10	2.6697E+10	2.5970E+10	3.2452E+10	4.5083E+10	5.2079E+10	3.5074E+10	3.0012E+10	1.9832E+10	1.0965E+10
56.23	4.7154E+09	7.2929E+09	1.6848E+10	1.6751E+10	2.3401E+10	3.6194E+10	4.5483E+10	3.6005E+10	3.7822E+10	2.9608E+10	2.0144E+10
64.94	1.7004E+09	3.1438E+09	9.3150E+09	9.4490E+09	1.4938E+10	2.5954E+10	3.6029E+10	3.3813E+10	4.2446E+10	3.7900E+10	2.9688E+10
74.99	4.5041E+08	1.0830E+09	4.3760E+09	4.5174E+09	8.2443E+09	1.6341E+10	2.5578E+10	2.8700E+10	4.2254E+10	4.2161E+10	3.6883E+10
86.6	7.0704E+07	2.5916E+08	1.6652E+09	1.7380E+09	3.7839E+09	8.7927E+09	1.5991E+10	2.1687E+10	3.7042E+10	4.0901E+10	3.9389E+10
100	2.0235E+06	3.3698E+07	4.7463E+08	4.8857E+08	1.3359E+09	3.8509E+09	8.5614E+09	1.4282E+10	2.8228E+10	3.4439E+10	3.6323E+10
115.48	1.9136E+07	2.0991E+07	9.6368E+07	8.6924E+07	2.9565E+08	1.2382E+09	3.7338E+09	7.9129E+09	1.8269E+10	2.4818E+10	2.8730E+10
133.35	2.6886E+07	3.6965E+07	3.8353E+07	2.8368E+07	1.4626E+07	2.1555E+08	1.1897E+09	3.4410E+09	9.6094E+09	1.4878E+10	1.9116E+10
153.99	1.8474E+07	3.3189E+07	4.7349E+07	4.1312E+07	1.8112E+07	1.4922E+06	2.0294E+08	9.9311E+08	3.7372E+09	7.0007E+09	1.0260E+10
177.83	6.9825E+06	1.7115E+07	4.3689E+07	4.1554E+07	4.3256E+07	2.3017E+07	2.2444E+06	9.3169E+07	8.1855E+08	2.2633E+09	4.0497E+09
205.35	1.0885E+06	4.2720E+06	2.5932E+07	2.4952E+07	4.4916E+07	4.7927E+07	2.6749E+07	6.6676E+05	0.0000E+00	3.2365E+08	8.9893E+08
237.14	1.2119E+05	3.7116E+05	1.0178E+07	8.6581E+06	2.7266E+07	4.9167E+07	4.2828E+07	7.4991E+06	0.0000E+00	0.0000E+00	0.0000E+00
273.84	1.3058E+05	2.4830E+05	2.5447E+06	1.3742E+06	9.7651E+06	3.1059E+07	3.4502E+07	1.3141E+07	0.0000E+00	0.0000E+00	0.0000E+00
316.23	3.6833E+05	5.7966E+05	3.1527E+05	1.1694E+04	1.2458E+06	1.2441E+07	1.7560E+07	1.2113E+07	1.8114E+05	0.0000E+00	0.0000E+00
365.17	6.9546E+05	1.0022E+06	6.4351E+05	3.0660E+04	1.3630E+02	2.6029E+06	4.4601E+06	8.0801E+06	6.0711E+05	0.0000E+00	0.0000E+00
421.7	8.2322E+05	1.1605E+06	8.9027E+05	1.0676E+05	9.9044E+03	3.1684E+05	1.0554E+05	4.1734E+06	1.2394E+06	0.0000E+00	0.0000E+00
486.97	7.2595E+05	1.0234E+06	8.9375E+05	2.0799E+05	2.3494E+04	2.0219E+04	0.0000E+00	1.7252E+06	1.2995E+06	0.0000E+00	0.0000E+00
562.34	5.3061E+05	7.3831E+05	7.3623E+05	2.8300E+05	4.6758E+04	2.8262E+04	0.0000E+00	5.1386E+05	6.8316E+05	1.0619E+04	0.0000E+00
649.38	3.7291E+05	4.6800E+05	5.6716E+05	3.3198E+05	1.0461E+05	7.1193E+04	1.3621E+04	0.0000E+00	0.0000E+00	0.0000E+00	0.0000E+00
749.89	3.0926E+05	3.2281E+05	4.6909E+05	3.5000E+05	1.8639E+05	1.5844E+05	6.1510E+04	7.3580E+03	0.0000E+00	0.0000E+00	0.0000E+00
865.96	3.0860E+05	2.9635E+05	4.4588E+05	3.4055E+05	2.5285E+05	2.7253E+05	1.5380E+05	4.5118E+04	0.0000E+00	0.0000E+00	0.0000E+00
1000	3.3062E+05	3.7784E+05	4.7212E+05	3.1789E+05	2.6900E+05	3.4515E+05	2.5644E+05	9.9543E+04	0.0000E+00	0.0000E+00	0.0000E+00

	HAB (mm)										
D_p (nm)	30	31	32	33	34	35	36	37	38	39	40
4.87	3.4612E+07	4.0826E+07	3.1626E+08	3.0786E+07	2.5566E+07	3.4918E+07	2.4073E+07	2.4962E+07	3.8550E+07	4.9787E+07	2.5571E+07
5.62	3.9234E+07	4.3757E+07	3.8220E+08	2.7498E+07	2.0697E+07	3.5369E+07	2.3468E+07	2.4314E+07	3.9421E+07	5.6610E+07	2.8285E+07
6.49	3.7085E+07	3.4780E+07	2.6537E+08	1.7397E+07	1.3462E+07	2.7934E+07	1.9511E+07	2.0381E+07	3.3497E+07	4.9292E+07	2.6878E+07
7.5	3.5389E+07	2.6481E+07	1.9011E+08	2.2391E+07	1.9198E+07	2.9438E+07	2.5391E+07	2.6114E+07	3.8704E+07	4.8470E+07	2.8747E+07
8.66	1.9064E+07	1.5201E+07	2.0196E+08	2.0689E+07	1.6081E+07	2.7621E+07	2.5186E+07	2.5468E+07	3.2358E+07	4.9429E+07	2.2236E+07
10	3.7670E+06	7.4216E+06	2.1370E+08	1.6101E+07	1.3371E+07	2.5147E+07	2.4890E+07	2.3266E+07	2.3228E+07	5.3355E+07	1.6759E+07
11.55	0.0000E+00	0.0000E+00	1.6540E+08	1.4589E+06	2.9956E+06	8.4409E+06	1.3253E+07	1.0627E+07	8.1681E+06	3.1314E+07	6.5477E+06
13.34	3.0835E+06	0.0000E+00	1.6971E+08	0.0000E+00	0.0000E+00	0.0000E+00	2.7550E+06	0.0000E+00	0.0000E+00	2.6376E+06	6.0777E+05
15.4	2.9736E+08	2.7596E+08	4.4880E+08	1.4088E+07	5.6406E+05	2.6657E+06	1.2017E+06	1.0119E+06	3.6384E+06	9.2794E+06	1.8567E+07
17.78	9.5365E+08	9.7765E+08	1.1277E+09	2.5300E+08	1.8001E+08	1.7919E+08	1.3849E+08	1.2514E+08	1.4981E+08	1.5343E+08	1.5371E+08
20.54	1.4965E+09	1.5855E+09	1.7047E+09	5.1730E+08	4.2641E+08	4.3328E+08	3.5768E+08	3.2188E+08	3.6618E+08	3.6826E+08	3.1681E+08
23.71	1.3539E+09	1.4746E+09	1.5902E+09	5.5757E+08	5.1878E+08	5.4341E+08	4.6842E+08	4.1947E+08	4.6033E+08	4.6329E+08	3.5638E+08
27.38	6.1646E+08	7.1271E+08	8.6089E+08	3.4866E+08	3.9081E+08	4.2939E+08	3.8791E+08	3.4517E+08	3.6270E+08	3.6871E+08	2.4498E+08
31.62	0.0000E+00	0.0000E+00	1.2470E+08	7.5894E+07	1.5366E+08	1.8492E+08	1.7861E+08	1.5760E+08	1.5513E+08	1.6109E+08	7.9489E+07
36.52	7.5980E+07	0.0000E+00	2.6040E+07	0.0000E+00	0.0000E+00	0.0000E+00	0.0000E+00	0.0000E+00	9.9615E+05	1.5863E+06	4.1584E+06
42.17	1.7230E+09	1.4296E+09	1.0490E+09	2.6855E+08	1.3957E+08	9.2251E+07	4.2231E+07	4.4712E+07	8.9268E+07	1.0357E+08	2.0990E+08
48.7	5.9578E+09	5.5447E+09	4.3105E+09	1.9810E+09	1.4914E+09	1.3265E+09	9.9746E+08	9.7454E+08	1.1826E+09	1.2423E+09	1.3771E+09
56.23	1.2508E+10	1.2335E+10	1.0011E+10	5.5288E+09	4.4769E+09	4.1801E+09	3.3571E+09	3.2340E+09	3.7500E+09	3.7174E+09	3.6364E+09
64.94	2.0026E+10	2.0587E+10	1.7320E+10	1.0548E+10	8.8454E+09	8.4568E+09	7.0080E+09	6.6969E+09	7.6190E+09	7.2856E+09	6.6850E+09
74.99	2.6567E+10	2.8285E+10	2.4605E+10	1.6001E+10	1.3734E+10	1.3338E+10	1.1275E+10	1.0713E+10	1.2043E+10	1.1227E+10	9.8646E+09
86.6	3.0149E+10	3.3169E+10	2.9829E+10	2.0427E+10	1.7861E+10	1.7559E+10	1.5063E+10	1.4251E+10	1.5871E+10	1.4509E+10	1.2324E+10
100	2.9587E+10	3.3644E+10	3.1329E+10	2.2458E+10	1.9964E+10	1.9835E+10	1.7223E+10	1.6238E+10	1.7940E+10	1.6137E+10	1.3313E+10
115.48	2.5063E+10	2.9530E+10	2.8576E+10	2.1411E+10	1.9341E+10	1.9406E+10	1.7036E+10	1.6017E+10	1.7562E+10	1.5570E+10	1.2501E+10
133.35	1.8082E+10	2.2202E+10	2.2477E+10	1.7640E+10	1.6204E+10	1.6423E+10	1.4572E+10	1.3668E+10	1.4870E+10	1.3000E+10	1.0155E+10
153.99	1.0778E+10	1.3959E+10	1.4976E+10	1.2384E+10	1.1601E+10	1.1896E+10	1.0682E+10	9.9946E+09	1.0777E+10	9.2811E+09	7.0289E+09
177.83	4.9699E+09	6.9807E+09	8.1475E+09	7.1854E+09	6.9112E+09	7.2052E+09	6.5703E+09	6.1290E+09	6.5302E+09	5.5214E+09	4.0178E+09
205.35	1.4962E+09	2.4692E+09	3.3266E+09	3.2020E+09	3.2207E+09	3.4610E+09	3.2353E+09	3.0019E+09	3.1367E+09	2.5840E+09	1.7670E+09
237.14	1.2435E+08	4.1821E+08	8.0233E+08	8.9293E+08	1.0023E+09	1.1626E+09	1.1443E+09	1.0485E+09	1.0519E+09	8.2787E+08	4.9692E+08
273.84	0.0000E+00	0.0000E+00	0.0000E+00	1.7708E+07	9.4227E+07	1.7393E+08	2.0722E+08	1.8048E+08	1.5556E+08	1.0733E+08	3.0603E+07
316.23	0.0000E+00	0.0000E+00	0.0000E+00	0.0000E+00	0.0000E+00	0.0000E+00	0.0000E+00	0.0000E+00	0.0000E+00	0.0000E+00	0.0000E+00
365.17	0.0000E+00	0.0000E+00	0.0000E+00	0.0000E+00	0.0000E+00	0.0000E+00	0.0000E+00	0.0000E+00	0.0000E+00	0.0000E+00	0.0000E+00
421.7	0.0000E+00	0.0000E+00	0.0000E+00	0.0000E+00	0.0000E+00	0.0000E+00	0.0000E+00	0.0000E+00	0.0000E+00	0.0000E+00	0.0000E+00
486.97	0.0000E+00	0.0000E+00	4.1079E+02	0.0000E+00	0.0000E+00	0.0000E+00	0.0000E+00	0.0000E+00	0.0000E+00	0.0000E+00	0.0000E+00
562.34	0.0000E+00	0.0000E+00	2.6604E+06	0.0000E+00	0.0000E+00	0.0000E+00	0.0000E+00	0.0000E+00	0.0000E+00	1.4926E+04	4.8319E+03
649.38	3.5275E+04	1.6845E+05	7.3142E+06	5.2713E+05	3.5978E+05	7.0966E+04	2.6465E+04	1.0577E+05	1.8682E+05	2.8405E+05	2.8696E+05
749.89	1.2216E+05	2.8604E+05	8.5433E+06	1.3372E+06	9.3547E+05	8.6697E+05	6.5404E+05	7.9625E+05	9.0699E+05	1.1055E+06	6.7511E+05
865.96	0.0000E+00	2.0739E+04	5.0166E+06	9.8719E+05	7.2127E+05	8.2212E+05	7.4038E+05	8.5933E+05	9.1650E+05	1.1008E+06	5.2787E+05
1000	0.0000E+00	0.0000E+00	0.0000E+00	0.0000E+00	0.0000E+00	2.5526E+04	2.0156E+05	2.7255E+05	2.3551E+05	3.2713E+05	3.6113E+04

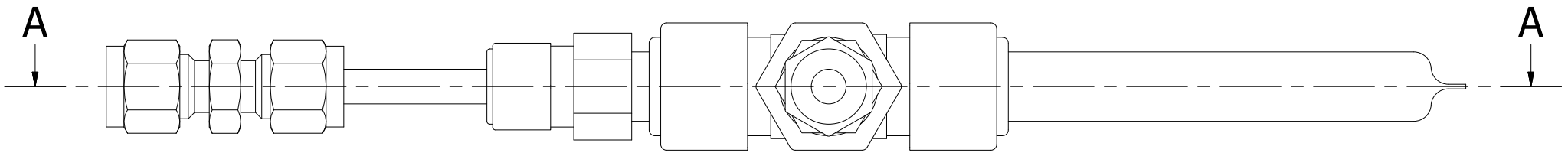

A-A (1 : 1)

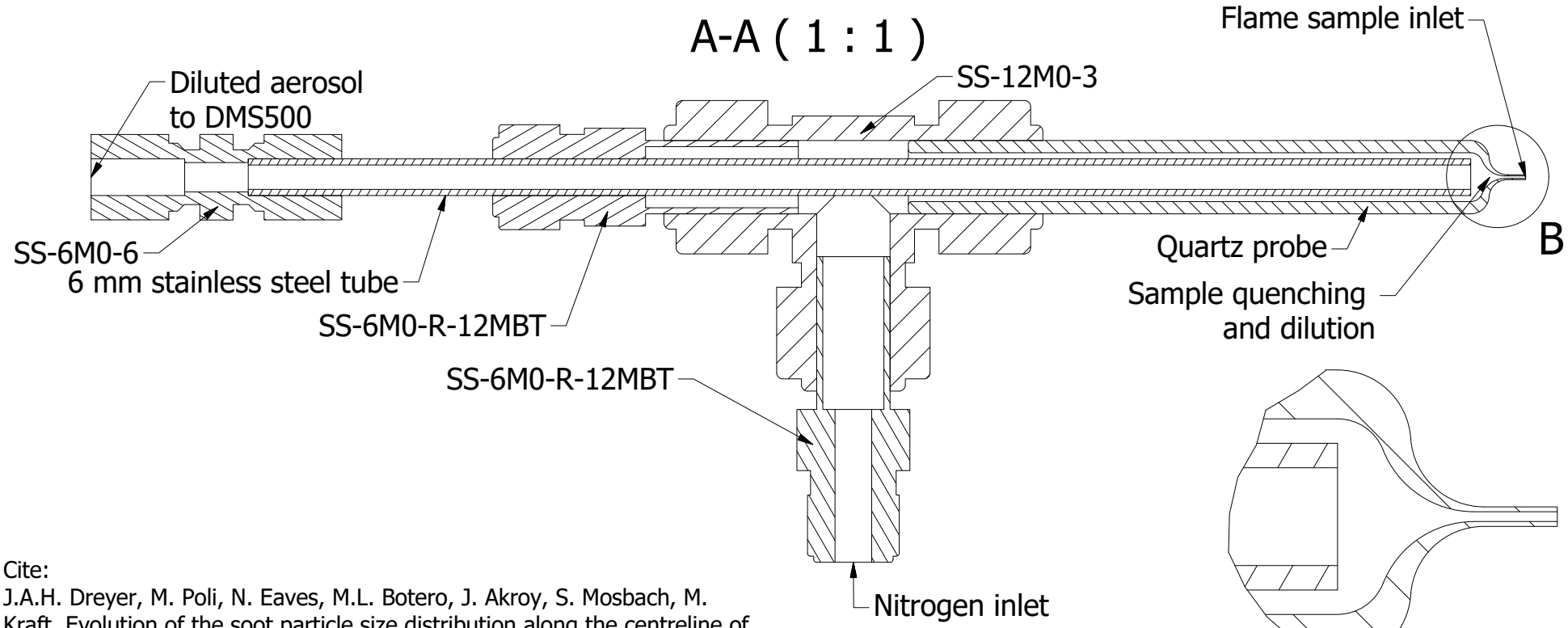

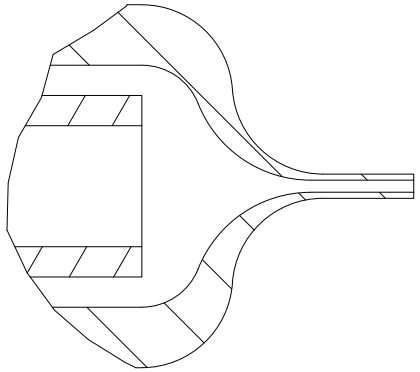

B (4 : 1)

Cite:
J.A.H. Dreyer, M. Poli, N. Eaves, M.L. Botero, J. Akroy, S. Mosbach, M. Kraft, Evolution of the soot particle size distribution along the centreline of a n-heptane/toluene co-flow diffusion flame

Designed by	Checked by	Approved by	Date		Date	
Jochen A.H. Dreyer					16/07/2018	

CoMo group, University of Cambridge	Aerosol sampling probe		
		Edition	Sheet 1 / 1